

Report No: DTS-00023-1390

SAR

12/12/08⁰³ Tsa

**ADVANCED RAILROAD WHEEL/RAIL INTERACTION FORCE
MEASUREMENT SYSTEM**

Jeffrey Everson
Susan MacPherson
Terrence Barnes
Wayne Hill
Foster-Miller, Inc.
350 Second Avenue
Waltham, MA 02451
781-684-4000

November 2000

Period: 9/14/99 - 06/30/00

Approved Final Report
Contract Number: DTRS57-99-C-00081
Contract Amount: \$99,701.00
Competitively Awarded
COTR: Dr. N. Thomas Tsai, RAD-20, FRA

Prepared for:

Federal Railroad Administration
Sixth Floor, Mail Stop 20
1120 Vermont Avenue, NW
Washington, DC 20590

FINAL PROJECT SUMMARY REPORT

PROJECT IDENTIFICATION INFORMATION

1. BUSINESS FIRM AND ADDRESS
Foster-Miller, Inc.
350 Second Avenue
Waltham, MA 02451
2. DOT SBIR PROGRAM
1999 Phase I
3. DOT CONTRACT NUMBER
DTRS57-99-C-00081
4. PERIOD OF PERFORMANCE
9/14/99 – 6/30/00
5. PROJECT TITLE
Advanced Railroad Wheel/Rail Interaction Force Measurement

SUMMARY OF COMPLETED PROJECT

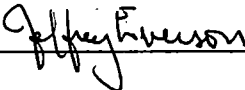
The data in this final report shall not be released outside the government without permission of the contractor for a period of four years from the completion date (4/28/00) of this project from which the data were generated.

The Phase I research into the development of a novel, cost effective and efficient wheel/rail interaction force measurement system demonstrated the ability to use silicon strain gauges, fabricated with MEMS manufacturing techniques, to measure the types of forces seen in car wheels. Silicon strain gauges, which operate based on their piezoelectric properties, were evaluated in the laboratory to compare their functionality to conventional resistive strain gauges. A design for the overall system concept is presented, including the foundation disk: the component that will hold all of the electronics and will be bonded to the wheel. Extensive epoxy evaluations, consisting of coupon load and fatigue tests, were performed in order to choose the best epoxy for this application. The program also demonstrated the ability to transmit data using RF data transmission hardware. A prototype transmission system contained within an electronics system a few inches in diameter was used to transmit data from the silicon gauges to a receiver attached to a data collection system. Evaluations proved that data could be reasonably transmitted by the prototype system over distances up to about 10 feet. The application of state-space analysis to the problem of system calibration is presented. The present methodology for measuring wheel/rail interaction forces involves extensive finite element modeling and precise gauge placement. The state space approach for calibration provides a simpler and quicker calibration methodology that will not require the precise gauge placement.

APPROVAL SIGNATURES

1. PRINCIPAL INVESTIGATOR/
PROJECT DIRECTOR (Typed)
2. PRINCIPAL INVESTIGATOR/
PROJECT DIRECTOR (Signature)
3. DATE

Jeffrey Everson, Ph.D.



7 November 2000

RIGHTS IN DATA - SBIR PROGRAM (MAR 1994)

These SBIR data are furnished with SBIR rights in accordance with FAR Clause 52.227-20 under Contract Number DTRS57-99-C-00081 (and subcontract N/A, if appropriate). For a period of four (4) years after acceptance of all items to be delivered under this contract, the Government agrees to use these data for Government purposes only, and they shall not be disclosed outside the Government (including disclosure for procurement purposes) during such period without permission of the contractor, except that, subject to the foregoing use and disclosure prohibitions, such data may be disclosed for use by support Contractors. After the aforesaid 4-year period, the Government has a royalty-free license to use, and to authorize others to use on its behalf, these data for Government purposes, but is relieved of all disclosure prohibitions and assumes no liability for unauthorized use of these data by third parties.

This notice shall be affixed to any reproductions of these data, in whole or in part.

EXPIRATION: November 2004

CONTENTS

Section	Page
1. INTRODUCTION	1
1.1 Limitations of Existing Technology	2
1.2 Background of Foster-Miller Concept.....	4
1.3 Phase I Objectives	5
2. SYSTEM DESIGN	6
2.1 Foundation Disk	6
2.2 MEMS Sensors	7
2.3 RF Transmission System	8
2.4 Power Systems	9
3. LABORATORY EVALUATIONS.....	12
3.1 Epoxy Testing	12
3.1.1 Test Coupons	12
3.1.2 Bonding Procedure	13
3.1.3 Load Testing	14
3.1.4 Fatigue Testing.....	15
3.2 Hardware Evaluation	16
3.2.1 Equipment Description	16
3.2.2 Test Fixture	17
3.2.3 Load Testing	20
3.2.4 Fatigue Testing.....	22
4. SENSOR CALIBRATION AND DATA EVALUATION METHODOLOGIES	33
4.1 Need for Calibration Methodology.....	33
4.2 Instrumented Wheel Set Calibration.....	33
4.3 Application of State Space Analysis.....	35
4.3.1 Applying State Space Analysis to Force Measurement.....	35
4.3.2 Example of State Space Analysis	38
4.3.3 Prior Use of State Space Analysis at Foster-Miller	44
4.4 Calibration Hardware	46
5. CONCLUSIONS	47

ILLUSTRATIONS

Figure	Page
1. FRA instrumented wheel set	3
2. IITRI/AAR instrumented wheel set	3
3. Foster-Miller approach for measuring wheel-rail interaction forces	4
4. Foster-Miller design, showing gauges, RF transmitter and power supply	6
5. Silicon strain gauge designed by AMMI	7
6. Foster-Miller design depicting wireless transmission between wheel-mounted strain gauges and a data collection computer	8
7. Method of powering the strain gauge devices by passing a coil-mounted on the wheel over a fixed, current, carrying coil	10
8. Method of powering the strain gauge devices by passing a coil mounted on the wheel past a fixed magnet	10
9. Drawing of epoxy test coupons	13
10. Aluminum plate (1/4 in. thick) test fixture for AMMI sensors	17
11. Installed silicon strain gauge supplied by AMMI	18
12. Annular flex circuit with RF electronics (left) and receiver connected to PC port of computer (right). Note the seven leads on the flex circuit for the seven silicon strain gauges	18
13. Detail of flex circuit electronics	19
14. Aluminum plate failed in shear while attempting to ramp the load to 20 kips	21
15. Position of operational gauge on test piece during ramp load	22
16. Silicon gauge tension test data up to around 4 kips	23
17. Conventional strain gauge tension test data up to 4 kips	24
18. Silicon gauge compression test data up to around 4 kips	25
19. Conventional strain gauge compression test data up to around 4 kips	26
20. New steel test fixture loaded into Instron machine	27
21. Results from silicon strain gauges in first cyclic test	29
22. Results from silicon strain gauges in second cyclic test	30
23. Results from MEMS gauges in third cyclic test	31
24. Results from standard strain gauges in third cyclic test	32
25. Force histories used in simulation	40
26. Vertical force predicted assuming orthogonality of sensors No. 1 and No. 2	41
27. State space prediction of vertical force	42
28. State space prediction of lateral force	43
29. Actual and predicted time traces of signal for sensor No. 8	44

TABLES

Table		Page
1.	Mixing ratio (by volume where not specified) and cure time for candidate epoxies	14
2.	Maximum strain ranking of the load samples	15
3.	Minimum error ranking of the samples	15
4.	Epoxy finalists and sample types used in fatigue tests	15
5.	Cycles achieved by each of the samples in the epoxy fatigue test	16
6.	Gain and phase error values used in simulation	39

PROGRAM SUMMARY

The Phase I research into the development of a novel, cost-effective and efficient railroad wheel/rail interaction force measurement system demonstrated the ability to use silicon strain gauges, fabricated with Micro Electrical Mechanical Systems (MEMS) manufacturing techniques, to measure the types of forces seen in rail car wheels. Silicon strain gauges, which operate based on their piezoelectric properties, were evaluated in the laboratory to compare their functionality to conventional resistive strain gauges.

A design for the overall system concept is presented, including the foundation disk: the component that will hold all of the electronics and will be bonded to the wheel. Extensive epoxy evaluations, consisting of coupon load and fatigue tests, were performed in order to choose the best epoxy for this application.

The program also demonstrated the ability to transmit data using RF data transmission hardware. A prototype transmission system contained within an electronics system a few inches in diameter was used to transmit data from the silicon gauges to a receiver attached to a data collection system. Evaluations proved that data could be reasonably transmitted by the prototype system over distances up to about 10 ft.

The application of state-space analysis to the problem of system calibration is presented. The present methodology for measuring railroad wheel/rail interaction forces involves extensive finite element modeling and precise gauge placement. The state space approach for calibration provides a simpler and quicker calibration methodology that will not require the precise gauge placement.

The railroad wheel/rail interaction force measurement system concept that was developed has the following advantages over the conventional system:

- Costly slip rings and the associated signal distortion can be avoided through the use of RF data transmission.
- Calibration time and cost for the wheel can be significantly reduced.
- The system can be used on existing service wheels, and can be calibrated in the field with portable calibration hardware.
- The overall cost of the system is anticipated to be significantly less than that of the conventional instrumented wheel set system.

1. INTRODUCTION

In an effort to improve rail transportation safety, the railroad industry periodically monitors the interaction forces between the wheels of the rail cars and the track. Variations in track geometry, truck suspensions and ballast stiffness can affect these interaction forces, which should be limited for safe operations of the rail vehicles to avoid possible derailment.

The method most often used by the industry to measure these forces is through an “instrumented wheel set” system. This is a set of rail car wheels instrumented with an array of strain gauges in a precise pattern. The service wheels are replaced with the instrumented wheel set and the tests are run. Data is transmitted from the wheel via a slip ring, a rotating contact mechanism, through the axle to the data collection system onboard the car. These instrumented wheel sets are expensive and labor intensive to manufacture, major effort is necessary to install the wheels onto the rail car, and extensive calibration of such a system is needed.

Foster-Miller, Inc. is developing a novel wheel/rail interaction force measurement system that will eliminate many of the downsides of the traditional instrumented wheel sets. The Foster-Miller concept addresses these problems through four key innovative features:

1. All-in-One System – The gauges, signal conditioning electronics, power supply, and data transmission equipment are all mounted onto a single foundation disk. The disk can be mounted directly to the service wheel, and can be done quickly and with minimal expense.
2. Advanced Sensors – The system employs silicon strain gauges, which are fabricated using MEMS (Micro Electrical Mechanical Systems) manufacturing techniques. The gauges will be embedded directly into the foundation disk, eliminating the need for tedious installation of individual gauges.
3. Wireless Data Transmission – The system uses an RF transmitter and receiver to send the data from the wheel to the data collection system onboard a railroad car. This eliminates the need for slip rings, which are presently used. An RF based system will provide a cleaner signal and more bandwidth than is available with a slip ring based system.
4. Calibration Methodology – The system will use a novel calibration system based on state space analysis. The processes can be performed rapidly by computer.

The Foster-Miller approach has the following benefits:

- Any service wheel can be instrumented while it is on the car, making the system much more adaptable to railroad operations, with a reduction of operating expenses.
- Accuracy and reliability will be improved by the elimination of the slip rings used in the current system.
- The use of state space analysis to improve the calibration methodology will reduce the time and cost required to perform the calibration of the system.

1.1 Limitations of Existing Technology

The most common way presently used to monitor the forces created by wheel/rail interaction is through the use of strain gauges. An instrumented wheel set is a set of rail car wheels that have been outfitted with an array of strain gauges to measure the vertical and lateral forces produced in the wheel. Presently, a slip ring is used to transmit the signals from the wheel to the car. A slip ring consists of silver graphite brushes running on electro-deposited silver rings and are housed in a sealed drum. The gauges are wired into the slip ring, and then to the data acquisition system through the axle of the truck. This procedure allows unwanted noise into the data stream, and restricts the total number of channels that can be read.

A number of different configurations of instrumented wheel sets are used. These are presented below.

- **FRA Instrumented Wheel Set** – This setup uses a standard AAR wheel with a concave conical wheel plate and a 1 in. minimum thickness. All surfaces of the plates are machined to ensure symmetry. The vertical force bridge consists of eight radial strain gauges arranged in a wheatstone bridge having two gauges per leg. The outputs of two identical bridges, out of phase by 45 deg, are summed. The lateral force bridge consists of eight radial strain gauges spaced around the field side of the wheelplate. Two identical bridges are wired 90 deg out of phase. The bridge arrangement cancels out the strain due to vertical force. A schematic of this type of wheel is shown in Figure 1.
- **IITRI/AAR Instrumented Wheel Set** – The arrangement of the strain gauge bridges on a standard AAR wheelplate is shown in Figure 2. Each of the three vertical bridges consists of 12 radial strain gauges with three gauges in each leg. Each bridge is used to sense vertical load within 60 deg sectors, which are centered 180 deg apart. The gauges on the opposite side of the plate are additive in the bridge. Each of the lateral bridges is composed of eight radial strain gauges on the inside plate, arranged with two gauges in each leg. Each bridge is used to sense the lateral load in two 90 deg sectors, which are centered 180 deg apart. The gauges in each of the 90 deg sectors are additive in the bridge.

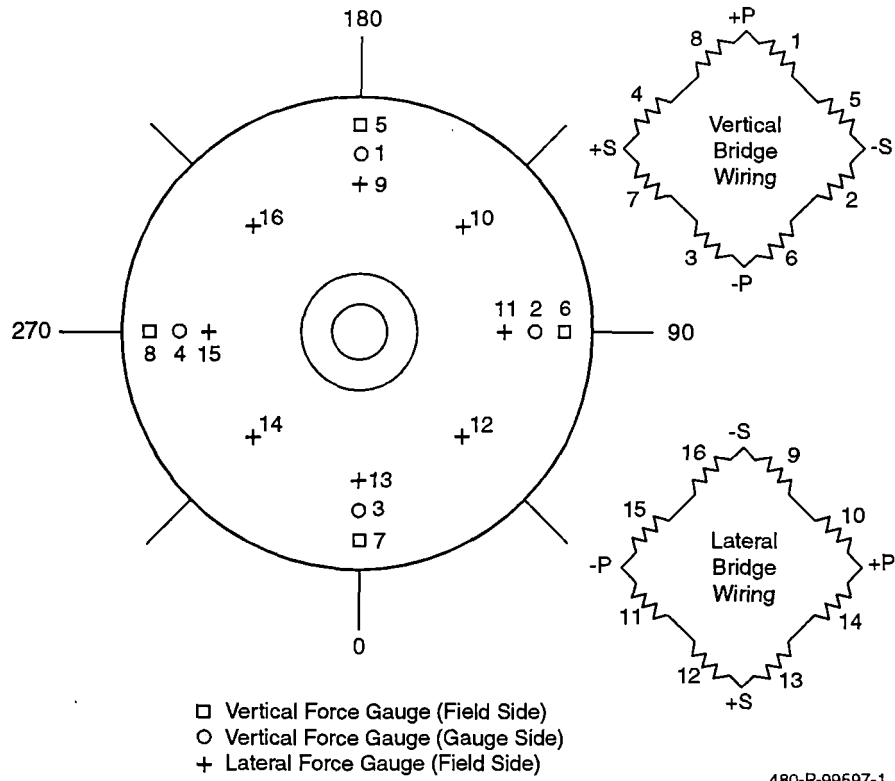


Figure 1. *FRA instrumented wheel set*

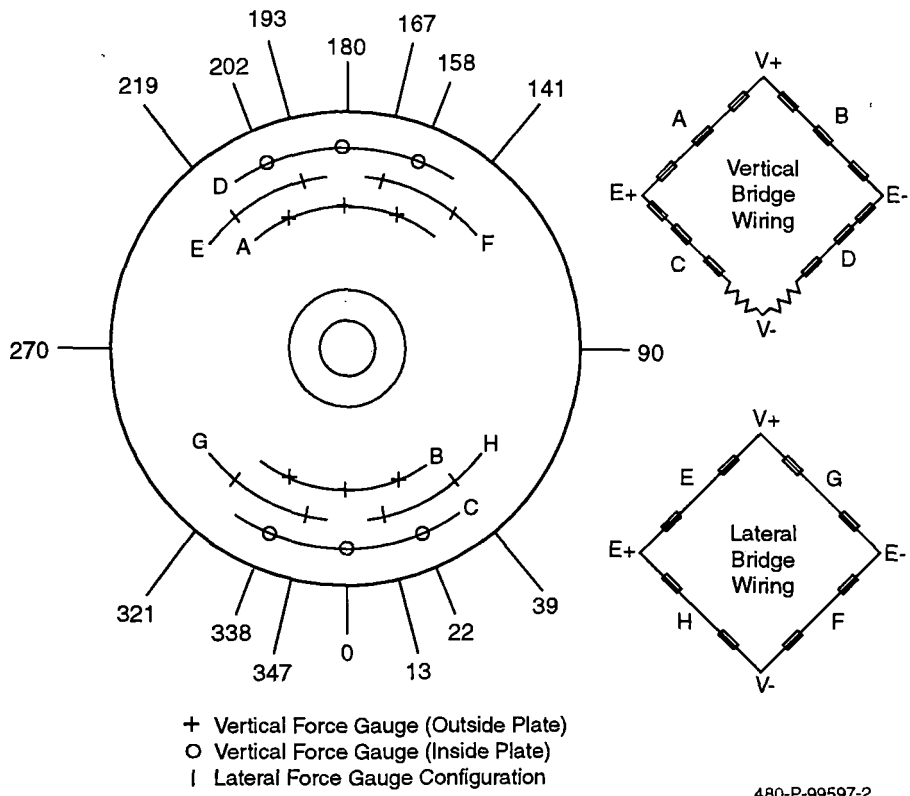
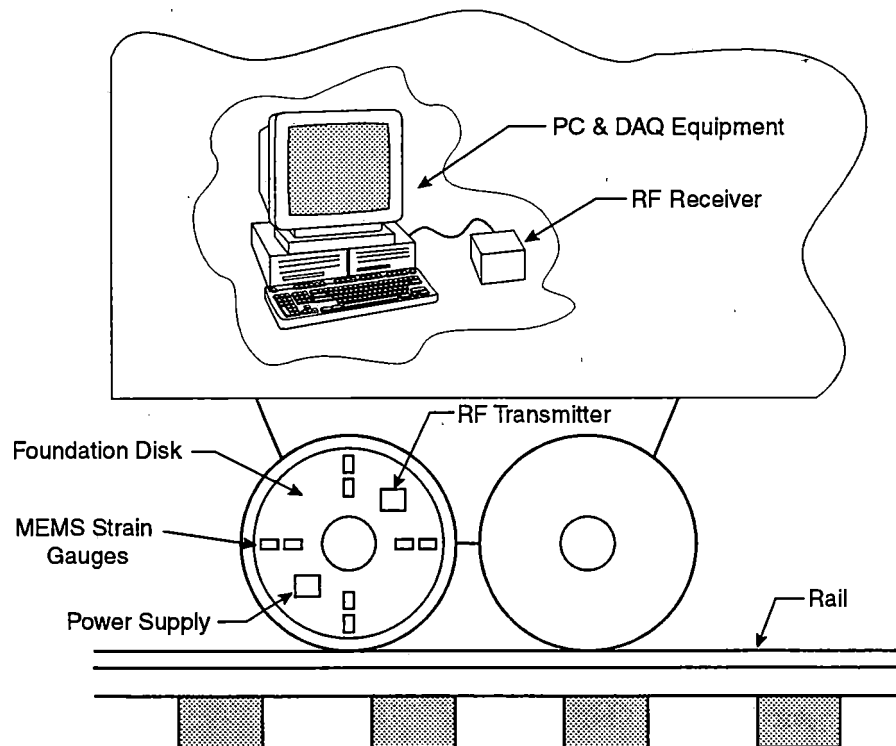


Figure 2. *IITRI/AAR instrumented wheel set*

- EMD/GM Instrumented Wheel Set – For this configuration, standard AAR wheels are again used. The vertical force bridge is composed of six strain gauges located 60 deg apart. A second set of six gauges is mounted, shifted around the circumference by 30 deg. The bridges are 90 deg out of phase with one another. The lateral force bridge is similar to the one used for the FRA wheel set.
- British Rail Spoked Wheel Set – The wheels in this configuration are specially forced and the 12 spokes formed by drilling and milling out intervening segments. A minimum of 12 spokes is necessary based on structural design calculations. An even number of spokes is required to provide symmetry in the design. A total of 96 gauges are mounted on the spokes.

1.2 Background of Foster-Miller Concept

The Foster-Miller design combines a number of innovations that together eliminate many of the limitations of the existing instrumented wheel set designs. The Foster-Miller wheel/rail interaction force measurement system is a self-contained package that can be bonded directly to service wheels, eliminating the need to replace the service wheels with the instrumented wheel set. The system uses RF technology to transmit data to a remote data collection system. The design also provides methodology for powering the gauges via batteries that can be recharged through inductive means. Figure 3 details the main components of the system.



480-P-99597-3

Figure 3. Foster-Miller approach for measuring wheel-rail interaction forces

The first innovation that the Foster-Miller design provides is the use of a separate disk that holds all of the gauges and electronics. The disk will be molded from a polyimide, a material traditionally used for strain gauge foundations. All of the silicon strain gauges, signal conditioning electronics, data transmission electronics, and battery systems will be contained in the disk. The disk will be mounted directly to the outer surface of the service wheel, eliminating the need to bring the car in for maintenance to switch the service wheels for instrumented wheels.

Another innovation is the use of RF technology to transmit the data from the silicon gauges to a data collection system on the car. The silicon gauges are particularly suited for this application because they can provide a higher sensitivity as compared with conventional strain gauges. This design will eliminate the need for the slip rings that are presently used. The system will also implement a novel power system by using batteries that are recharged through an induction system that is powered by the rotation of the wheel past a stationary magnet.

Finally, the Foster-Miller design provides a novel calibration system that has the potential to reduce the time, cost, and effort required to create and to calibrate an instrumented wheel set. This methodology is based on the use of state space analysis, and would eliminate the need for extensive finite element modeling and precise location of the strain gauges.

1.3 Phase I Objectives

The basic Phase I program goals are to demonstrate the feasibility and practicality of the innovation and to address any significant technical hurdles. In the Phase I proposal, these goals were to:

- Develop a new cost-effective and efficient wheel/rail interaction force measurement system with advanced sensors and data transmission methods.
- Demonstrate that silicon strain gauges can be used to measure strain in wheel configurations and their compatibility with the RF transmission system.
- Design a bondable platform for the silicon strain gauges that provides accurate strain transfer between the wheel and the gauges.
- Develop a calibration concept that would reduce the complexity of the existing calibration process.

2. SYSTEM DESIGN

The first portion of this program focused on the conceptualization of the system design. This included providing design specifications for each component of the system, including the foundation disk, gauges, signal conditioning and data transmission systems, and the system power. The specifics of these individual components are described in detail in the sections below.

2.1 Foundation Disk

The entire wheel/rail interaction force measurement system will be contained in a single disk that can be bonded directly to the outer surface of the rail car wheel. The disk will contain all of the silicon gauges, the RF hardware, and the power source for the gauge excitation and data transmission. A schematic of the disk is shown in Figure 4.

The disk will be made of polyimide, which is a material presently used for conventional strain gauge foundations. This approach will allow all of the circuitry to be embedded directly into the disk. The polyimide can be molded into any desired shape. A prototype polyimide ring

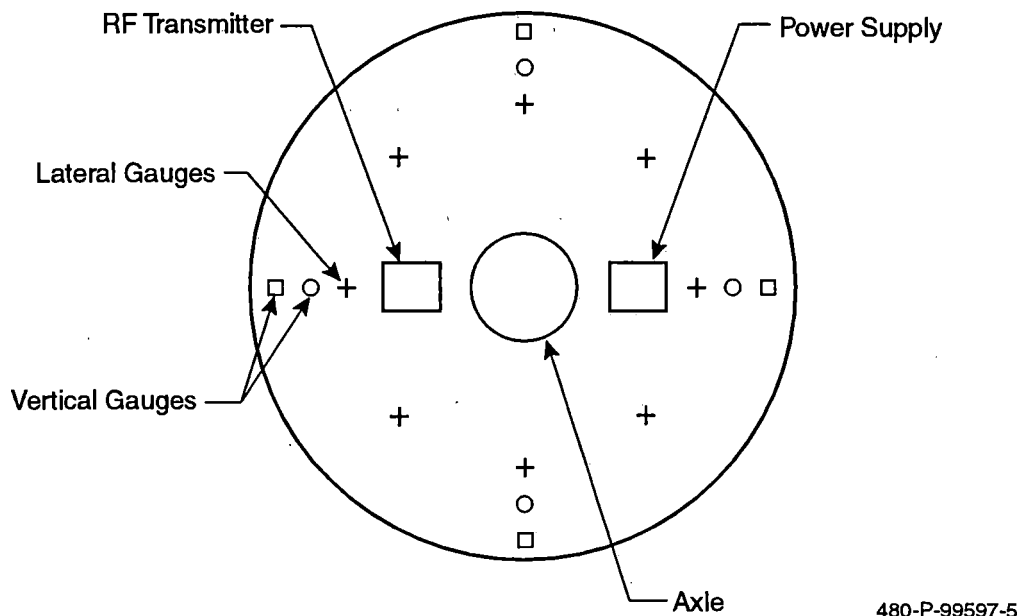


Figure 4. Foster-Miller design, showing gauges, RF transmitter and power supply

with embedded electronics was obtained from AMMI (Advanced Micro Machines, Inc.), Cleveland, OH, for test purposes during this program. This specific ring and its associated hardware are described further in subsection 3.2.1.

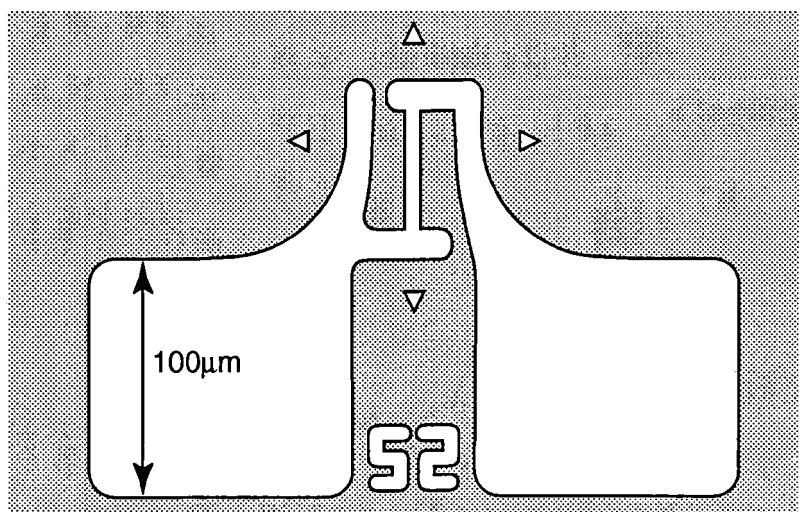
An important part of the design is the interface between the disk and the wheel. In order to measure the strain in the wheel accurately, there must be an interface that can transfer strain efficiently between the two components. The best option to attach the disk to the wheel is to use a high strength, high stiffness epoxy. An epoxy would create a uniform bond between the wheel and the disk, and provide good strain transfer between the two surfaces. To create an even bond line, micro beads could be added to the epoxy when it is mixed to create a consistent bond thickness. Standard off-the-shelf epoxies were evaluated for this application and are discussed in subsection 2.3.

2.2 MEMS Sensors

For this project the use of silicon strain gauges, made according to MEMS microfabrication techniques, was examined. A diagram of a silicon strain gauge is depicted in Figure 5, a design generated by AMMI.

These gauges are extremely small sensors fabricated from silicon, utilizing surface machining similar to that used for computer chip manufacturing. Employed for a number of different applications, such as pressure, temperature, vibration, and strain measurements, silicon strain gauges support a number of industrial and research applications, but have not yet been applied to the railroad industry.

Silicon strain gauges fabricated with MEMS technology are becoming more prevalent. The initial development costs of the gauges can often be high, but once the gauge has been developed, it can be mass-produced very cheaply. In addition, as development methodologies improve, the initial costs will fall, and such gauges will become more widely available.



481-P-99597-3

Figure 5. *Silicon strain gauge designed by AMMI*

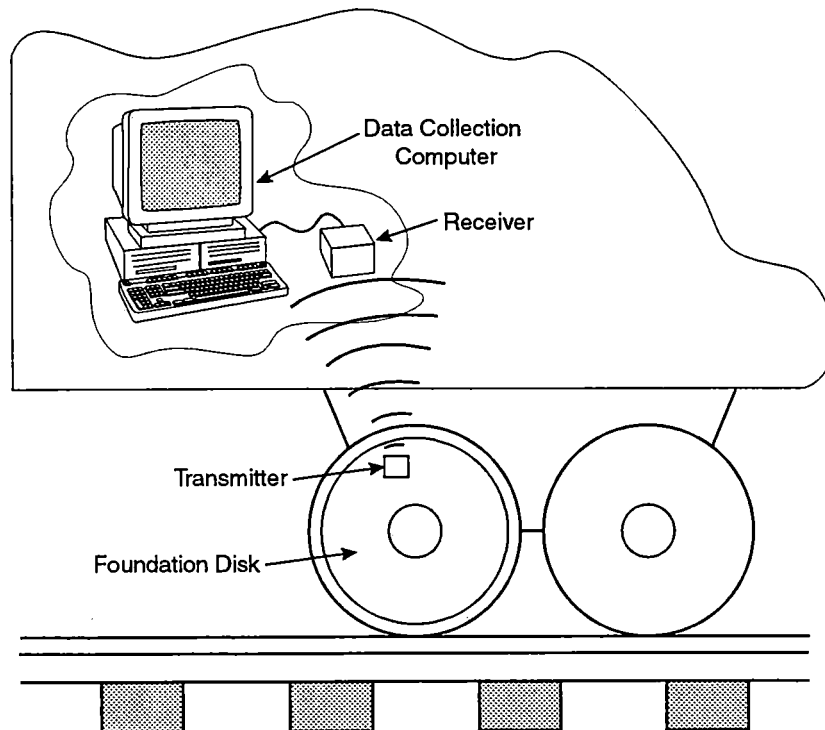
Silicon strain gauges can have gauge factors from 60 to 100, whereas metal foil strain gauges have factors of approximately 2. A larger gauge factor provides greater sensitivity to detect for the presence of strains. For example, if a metal foil strain gauge registers 0.1Ω for a given strain, then a silicon strain gauge would measure 10Ω for the same strain when its gauge factor is 100. Since a larger change in resistance is measured, the system can more accurately measure smaller strains, and resolve those strains to smaller levels.

Several silicon strain gauges were obtained for evaluation during this program. Descriptions of these evaluations and their results are presented in subsection 3.2.

2.3 RF Transmission System

One of the disadvantages of the present instrumented wheel set is the necessity of using a slip ring to transmit the data from the gauges to the data acquisition system. This approach generates a noisy connection, and the number of possible channels is limited by the size of the slip ring. The slip ring temperature also has to be regulated with a heater during operation.

Foster-Miller's system eliminates the need for this component by replacing it with a wireless system, as shown in Figure 6. The data is transmitted via radio waves. Located directly on the foundation disk on the wheel, the transmitter broadcasts signals from the strain gauges so that the receivers onboard the train can pick up the signals for data reduction. The power supply for the transmitters is located on the foundation disk as well.



480-P-99597-4

Figure 6. *Foster-Miller design depicting wireless transmission between wheel-mounted strain gauges and a data collection computer*

The electronic system consists of an IC chip, RF chip and an antenna. All of these components can be embedded in the foundation disk during fabrication and assembly procedures. Contained within the IC chip are interfacing electronics for the strain gauges, A/D conversion circuitry, and a multiplexer. The strain measurement, in the form of a DC off-set voltage, can be transmitted to a PC via the RF module and antenna. A carrier frequency of 900 MHz has been used, and is within the unlicensed band. The PC can be equipped with software to permit manipulation, visualization and analysis of the strain data.

2.4 Power Systems

The use of batteries, even lithium batteries, to power the sensor/transmitter would require frequent replacement. Once the foundation disc is bonded to the wheel, it is desirable that normal disc maintenance tasks such as accessing onboard memory to collect data, or to change batteries, are minimized or avoided. The wireless measurement system must be intrinsically low-maintenance. To accomplish this requirement, a power management system must be an integral part of it.

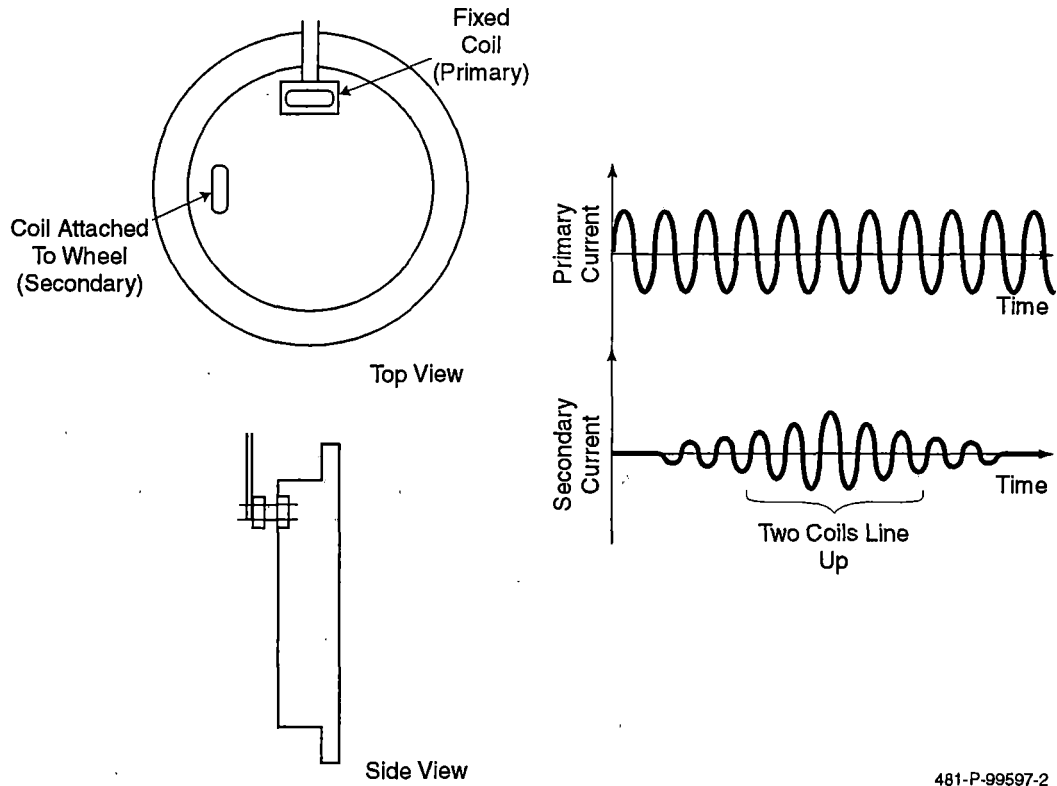
This power management system would perform three important tasks. These are: 1) manage the use of power, 2) recharge an onboard battery, and 3) sense when maintenance is needed.

Manage the use of power. The system is to know when the sensor is not in use and shut down the transmitter and enter a low-power "sleep" mode. Achieving this function would not only conserve power, but also prevent the unnecessary transmission of RF signals. Such circuitry readily exists and is used, for example, to conserve power in notebook computer displays.

Provide power to an onboard rechargeable battery. One simple way to accomplish this is illustrated in Figure 7. A small fixed coil of wire is placed adjacent to the wheel. AC current through this coil effectively causes electromagnetic radiation to be transmitted to the wheel. A second coil in the sensor assembly, on the wheel, picks up the radiated energy when it comes into the vicinity of the transmitter coil. There it is rectified and used to charge the battery. As in a transformer, energy is inductively transferred from the primary coil to the secondary in the sensor.

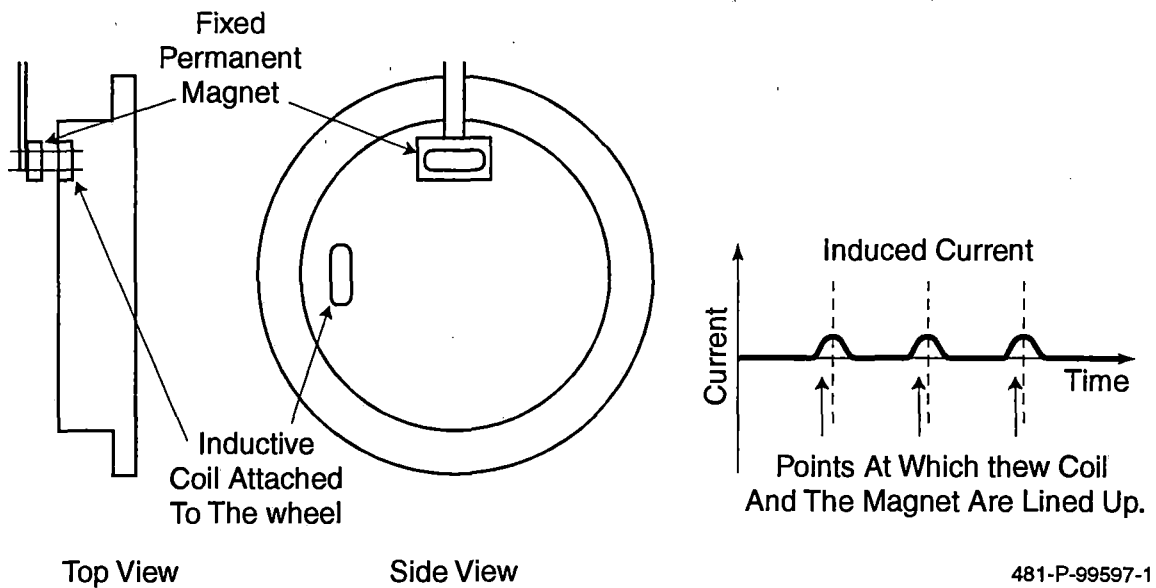
Another simple (and passive) technique would be to replace the primary coil with a permanent magnet (Figure 8). The motion of the secondary coil passing close by the magnet would induce a small current. Although small, there would be sufficient current to trickle charge the onboard battery. The energy to charge the battery ultimately comes from the rotational kinetic energy of the wheel. The advantage of this technique is that it is passive and requires no active excitation from outside the sensor.

Sense when maintenance is needed. Proper normal operation of the power management system may easily be monitored. For example, the inability to achieve sufficient battery charge rate may indicate the need for maintenance or service. This fact may then be transmitted to the receiver and thus alert the data monitoring system. Thus, maintenance is only performed when needed, eliminating the requirement of regular routine service checks.



481-P-99597-2

Figure 7. *Method of powering the strain gauge devices by passing a coil-mounted on the wheel over a fixed, current, carrying coil*



481-P-99597-1

Figure 8. *Method of powering the strain gauge devices by passing a coil mounted on the wheel past a fixed magnet*

For the prototype testing described later in this report, a power supply was used to provide power to the silicon strain gauges and the data transmission system. The innovative power system designs described here were not constructed as part of this Phase I program, but their development would be an integral part of the Phase II program.

3. LABORATORY EVALUATIONS

To validate the principles laid out in the concept of the wheel/rail interaction force measurement system, a series of laboratory evaluations were performed. The two main goals of these evaluations were to select an appropriate epoxy that will be used to bond the foundation disk to the wheel of a rail car, and to evaluate the silicon strain gauges and associated hardware supplied to Foster-Miller by AMMI. The specifications, procedures, and results for these tests are described in the section below.

3.1 Epoxy Testing

The design of the wheel/rail interaction force measurement system requires a strong epoxy that can create a vibration resistant, high stiffness, and weatherproof bond to adhere the foundation disc to the railroad wheel. A number of different epoxies were examined to determine which has the best response under the loads to be expected in a railroad environment. Test coupons were created using each of the potential epoxies and evaluated in an Instron tensile testing machine for stiffness response and failure loading scenarios.

For this measurement system, it is necessary to use an epoxy that is strong enough to withstand the railroad environment, and provide good strain transfer between the wheel and the foundation disk. Good strain transfer will allow for accurate measurement of the wheel/rail interaction forces. Strain gauges were installed onto the test coupons to measure the strain during testing.

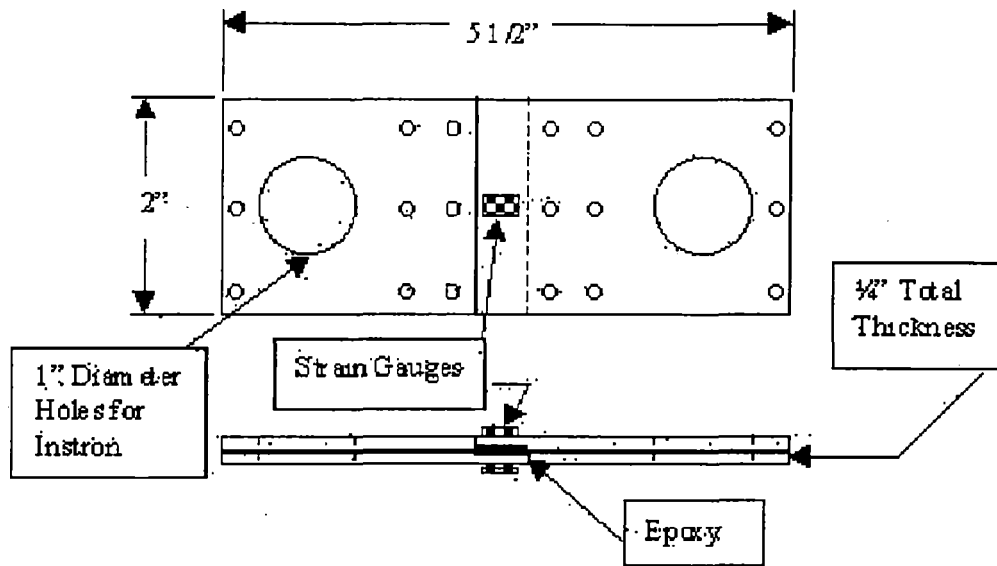
Five high strength epoxies were evaluated during these tests. These were:

- Hysol EA 9396.
- Hysol 9460F.
- 3M DP-10.
- Loctite E-20 NS.
- Loctite E90 FL.

Two different types of tests were run using the epoxy test coupons: load-failure tests, and fatigue tests.

3.1.1 Test Coupons

Each of the test coupons is identical, and has dimensions as shown in Figure 9. The coupons were sized so that they fit properly into the Instron machine and that they themselves will not fail



522-DTS-00023-1

Figure 9. Drawing of epoxy test coupons

during testing, allowing for proper analysis of epoxy properties. Each coupon consists of four parts, two pieces (2 in. x 2-1/2 in.) and two additional pieces (2 in. x 3 in.). The manner in which these pieces are joined can be seen in the side view of the coupon in Figure 9.

3.1.2 Bonding Procedure

The following is a summary of the procedure that was used to bond the two halves of each test coupon together.

- Clean and degrease all coupon components.
- Bond coupon parts together to create coupon halves.
- Tape bond wires in place across the bond surface of one coupon half per coupon assembly.
- Mix epoxy parts at proper ratio. (See Table 3-1 for epoxy mix ratios.).
- Apply epoxy to the bond surface of the coupon half with bond wires.
- Put second coupon half in place, mating the two bond surfaces.
- Apply two C-clamps to the coupon to hold the halves in place during curing.
- Allow epoxy to cure for appropriate time. (See Table 1 for cure times.)

Table 1. *Mixing ratio (by volume where not specified) and cure time for candidate epoxies*

Epoxy Type	Mixing Ratio	Cure Time at Room Temperature
Hysol 9460F	1:1	3 days
Hysol EA 9396	100:30 (by weight)	5 days
Loctite E90FL	1:1	24 hr
Loctite E20NS	2:1	24 hr
3MDP-110	1:1	24 hr

Despite the long cure times shown in Table 1, using heat to accelerate the curing process can dramatically shorten these times. Cure times can be reduced, depending on the epoxy, to periods on the order of a half-hour.

3.1.3 Load Testing

Load-failure tests can determine the maximum shear stress that the epoxy can handle before failure. Forty-five samples (five epoxies, three bond thicknesses, and three samples per epoxy/bond thickness combination) were evaluated. The three bond thicknesses were 0.002, 0.006, and 0.009 in. Each sample was pulled to failure at a rate of 0.05 in./min. The force, displacement, and strain for each sample was recorded at a rate of 0.5 Hz, which is adequate for this type of slow ramping. A strain gauge was mounted on each side of the test coupon. The coupon was mounted vertically into the Instron machine. The strain gauge on the half of the coupon that was closest to the load cell was used as the reference strain and the gauge opposite side of the bond represented the transferred strain.

The methodology for choosing epoxy finalists included balancing load capability and strain transfer. It is important that the epoxy can withstand the strain levels that would be encountered in the railroad wheel environment. It is also necessary that the strain is accurately transferred from the wheel to the gauge through the epoxy.

Since three samples were tested for each epoxy/bond combination, those three results were averaged. The samples were ranked by maximum strain at failure and strain transfer error. Maximum strain is defined as the strain at which failure occurred. Strain transfer error is the difference in the two strain gauges divided by the reference strain. Each of the sample types was ranked based on the test results, with 1 being the best and 15 being the worst. The rankings for all of the samples are shown in Tables 2 and-3.

Most of the high strain ranks were disqualified for having high errors, and those with low errors often had very low maximum strains. For example, the Hysol EA 9396 0.006 in. sample had the highest average maximum strain, but exhibited the second highest error. The three best samples are shown in Table 4.

Table 2. Maximum strain ranking of the load samples

	Bond Thickness		
	0.002 in.	0.006 in.	0.009 in.
Hysol EA 9396	12	1	14
Hysol 9460 F	4	5	7
3MDP-110	13	2	3
Loctite E-20NS	15	11	8
Loctite E-90FL	9	10	6

Table 3. Minimum error ranking of the samples

	Bond Thickness		
	0.002 in.	0.006 in.	0.009 in.
Hysol EA 9396	13	14	12
Hysol 9460 F	10	7	5
3MDP-110	2	15	6
Loctite E-20NS	4	3	9
Loctite E-90FL	1	8	11

Table 4. Epoxy finalists and sample types used in fatigue tests

Epoxy	Bond	Maximum Strain Rank	Minimum Error Rank
3MDP-110	0.009 in.	2nd of 15 samples	6th of 15 samples
Hysol 9460F	0.006 in.	5th of 15 samples	7th of 15 samples
Hysol 9460F	0.009 in.	7th of 15 samples	5th of 15 samples

The results shown above balance the two epoxy qualifications. These three epoxies were subjected to fatigue testing. Three samples of each of the epoxy/bond combinations were evaluated under cyclic loading in the Instron tensile testing machine.

3.1.4 Fatigue Testing

After the load failure tests were completed and finalists were selected, those finalists were evaluated for their ability to withstand cyclic loading, which is more representative of the railroad environment.

For each of the finalists that were chosen after the tension to failure tests (Table 4), three samples of each were created for cyclic testing. The test coupons used were identical to those used in the tension to failure tests. The bonding process was also the same.

Each of the coupons was loaded slightly in tension in the Instron machine. The coupons were cycled between 75 and 375 lb at a rate of 1 Hz. This load range was chosen based on the

performance of the tension to failure test coupons. Each of the coupons was cycled for 10,000 cycles, unless failure occurred before that time. Data was collected for the load and displacement values, as well as from the two strain gauges on each coupon.

Table 5 shows the cycle counts achieved for each of the coupons. It is immediately obvious that the 3M DP-110 did not perform well under cyclic loading, despite its performance during the tension to failure testing. Each of the samples failed far before 10,000 cycles. All of the Hysol 9460F samples achieved 10,000 cycles without failure.

It was concluded that the Hysol 9460F epoxy is the most appropriate epoxy for the foundation disk application. Since the two bond thicknesses behaved similarly during the cyclic loading testing, and also similarly during the tension to failure tests, the thinner of the two bond thicknesses will be chosen to reduce the amount of epoxy required.

3.2 Hardware Evaluation

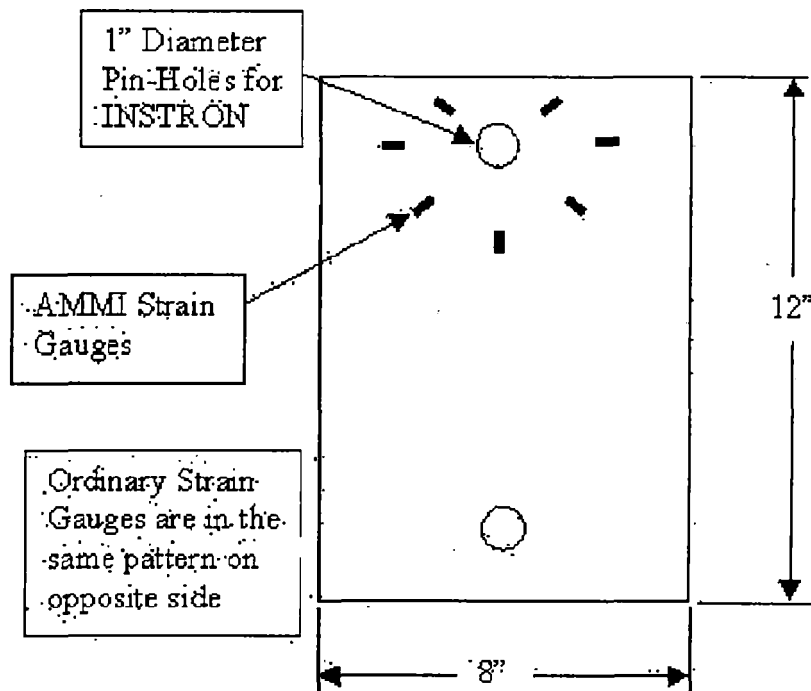
The silicon strain gauge sensors must be able to accurately measure the strains in the railroad wheels. Additionally, the RF equipment must be capable of transmitting strain gauge data successfully to the onboard computer. For these reasons, the functionality of the silicon gauges was compared to that of regular strain gauges. To do this, the sensors were bonded to an aluminum plate (Figure 10) to be used as the foundation. Because aluminum can be strained easily, a large load was not required. Thus, good quality strain data was collected. Two different types of tests were run using the silicon gauges. A ramp load was applied first as a preliminary evaluation and then a cyclic load was applied to simulate railroad wheel loads. Both tests were used to compare the output from each type of sensor.

3.2.1 Equipment Description

A prototype measurement system, developed by AMMI, was used for the evaluation portion of this program. This prototype was an off-the-shelf system developed for use monitoring

Table 5. Cycles achieved by each of the samples in the epoxy fatigue test

Sample	Cycle Count
3MDP-110 -0.009 in.	1255
3MDP-110 -0.009 in.	780
3MDP-110 -0.009 in.	Failed Immediately
Hysol9460F -0.006 in.	10,000 (no failure)
Hysol9460F -0.006 in.	10,000 (no failure)
Hysol9460F -0.006 in.	10,000 (no failure)
Hysol9460F -0.009 in.	10,000 (no failure)
Hysol9460F -0.009 in.	10,000 (no failure)
Hysol9460F -0.009 in.	10,000 (no failure)



522-DTS-00023-2

Figure 10. Aluminum plate (1/4 in. thick) test fixture for AMMI sensors

helicopter rotor gears, and was not tailored to the interaction force measurement problem. In a Phase I program, the development of a custom system was not feasible, however, the AMMI system somewhat matched the requirements to prove the fundamental concept of the design.

The AMMI prototype system consists of three parts:

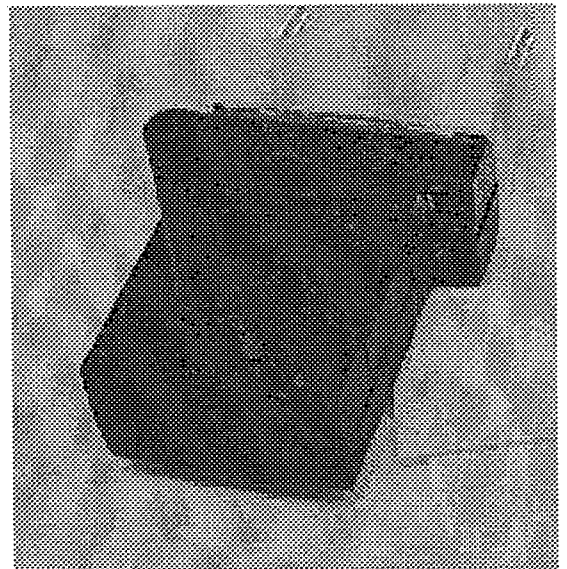
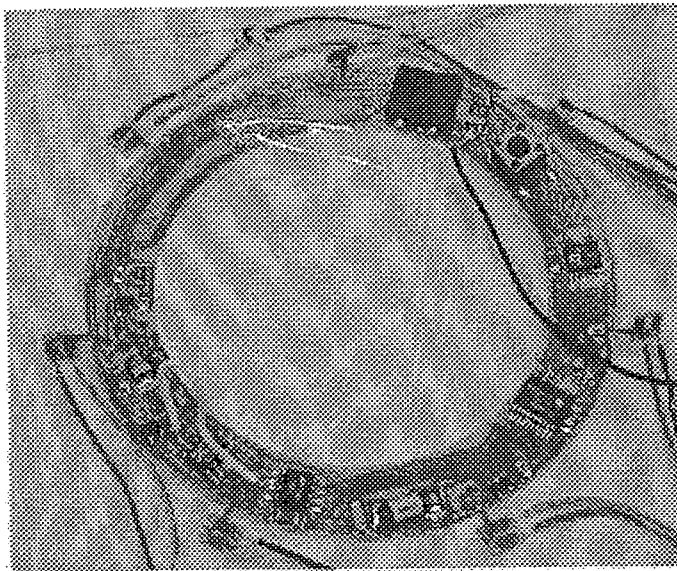
- Silicon strain gauges fabricated with MEMS manufacturing techniques (Figure 11).
- A polyimide flex circuit ring containing the signal conditioning electronics, multiplexer, and transmission antenna (Figure 12, Figure 13).
- An RF receiver that plugs into the parallel port of a PC and receives data from the flex circuit's transmitter (Figure 12).

3.2.2 Test Fixture

The silicon gauges were bonded in a circular pattern around one of the pinholes of the aluminum plate using M-Bond strain gauge adhesive (Figure 10). The sensors were then connected to the flex circuit, which was at a separate location, and not attached to the plate. The wires were soldered with "Kester Flux Core Solder."

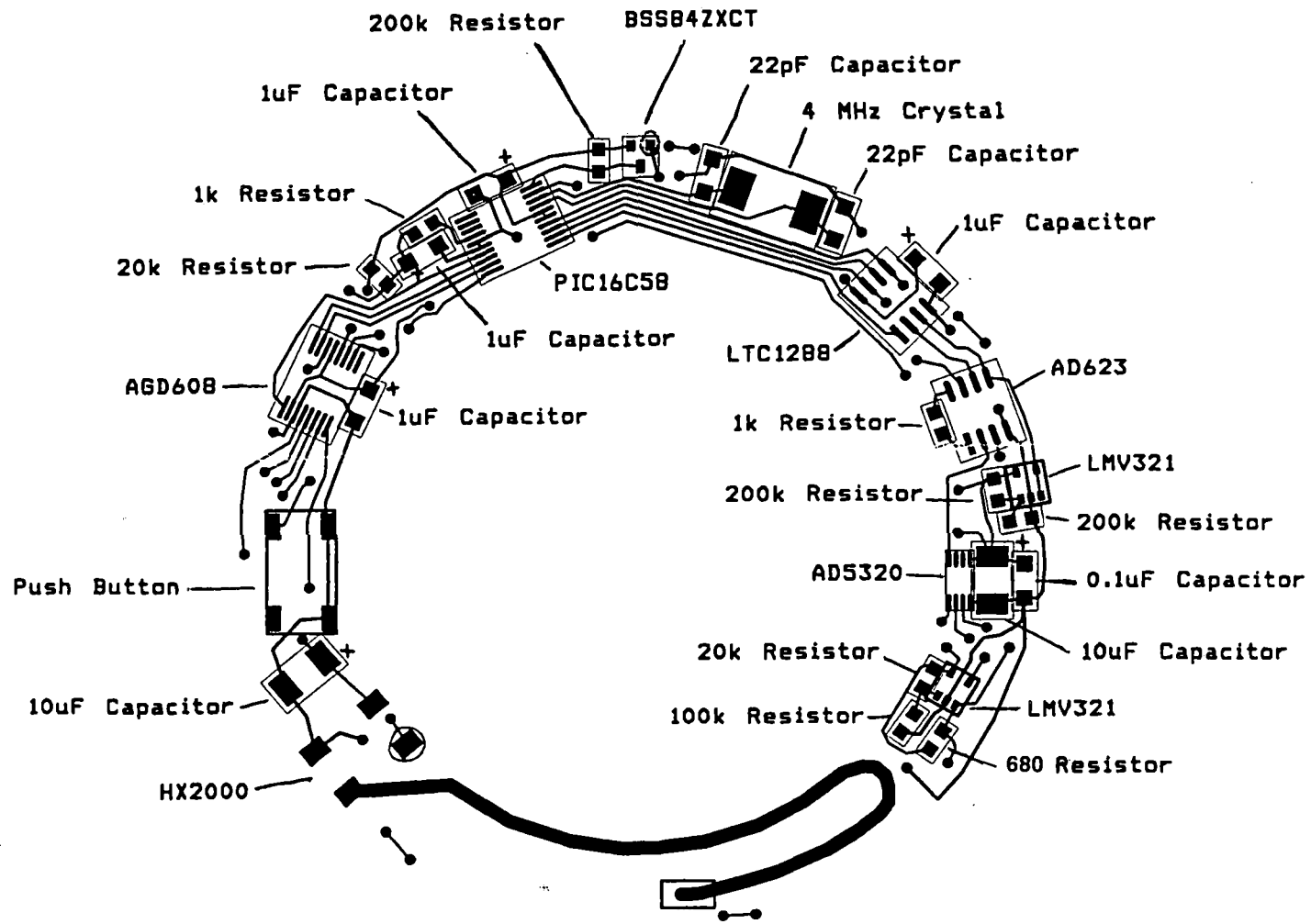


Figure 11. *Installed silicon strain gauge supplied by AMMI*



00A-1531

Figure 12. *Annular flex circuit with RF electronics (left) and receiver connected to PC port of computer (right). Note the seven leads on the flex circuit for the seven silicon strain gauges*



522-DTS-00023-3

Figure 13. Detail of flex circuit electronics

The conventional strain gauges were placed in a similar pattern, on the opposite side, for comparable data between the two gauge types. The data is comparable if the plate does not buckle under the compressive load from the Instron. It was found that the buckling load was around 29 kips, so the loading was programmed not to exceed this value in order for the data to be useful. These gauges were then connected to the data acquisition device.

3.2.3 Load Testing

A ramp load was applied to the fixture as a preliminary test to see the response of the hardware and to observe how it compares with the output of the standard strain gauges. Since data acquisition program could not be used at the same time for both types of strain gauges, each test had to be performed twice to record data from each type of device.

The basic procedure in performing the load test on the measurement system is as follows:

- Place the plate in the Instron machine and apply light load to hold the plate in place.
- Apply the pre-programmed ramp loading to the specimen.
- Press the button on the flex circuit to activate the RF transmitter. It stays active for about 30 sec.
- After the loading program has ended, enable the data acquisition program for the standard strain gauges.
- Apply the same pre-programmed ramp loading to the specimen.
- After the loading program has ended, stop the data acquisition program.

The ramp load was applied to the plate up to around 10 kips tension initially. Then the plate was subjected to a ramp load of 10 kips compression, which is significantly less than the calculated buckling load. Another experiment was attempted where the plate would undergo a tensile ramp loading of 20 kips but the plate failed in shear around one of the pinholes (Figure 14). This load was applied at a rate of 333 lb/sec. Data was taken at a rate of 50 Hz.

The output of the silicon gauges is a normalized voltage on a scale of zero to three. As a specimen is being strained, a graph is shown on the computer screen indicating the output voltages from the channels. These voltages were later converted to strain values. One channel provided satisfactory data, while the other six channels required repairs that were prohibitively expensive to make. The equation to convert the output from voltage to strain is:

$$\epsilon_n = \frac{-2R_i(D_n - D_i)}{G(R_{gn})(GF_n)} \quad (1)$$

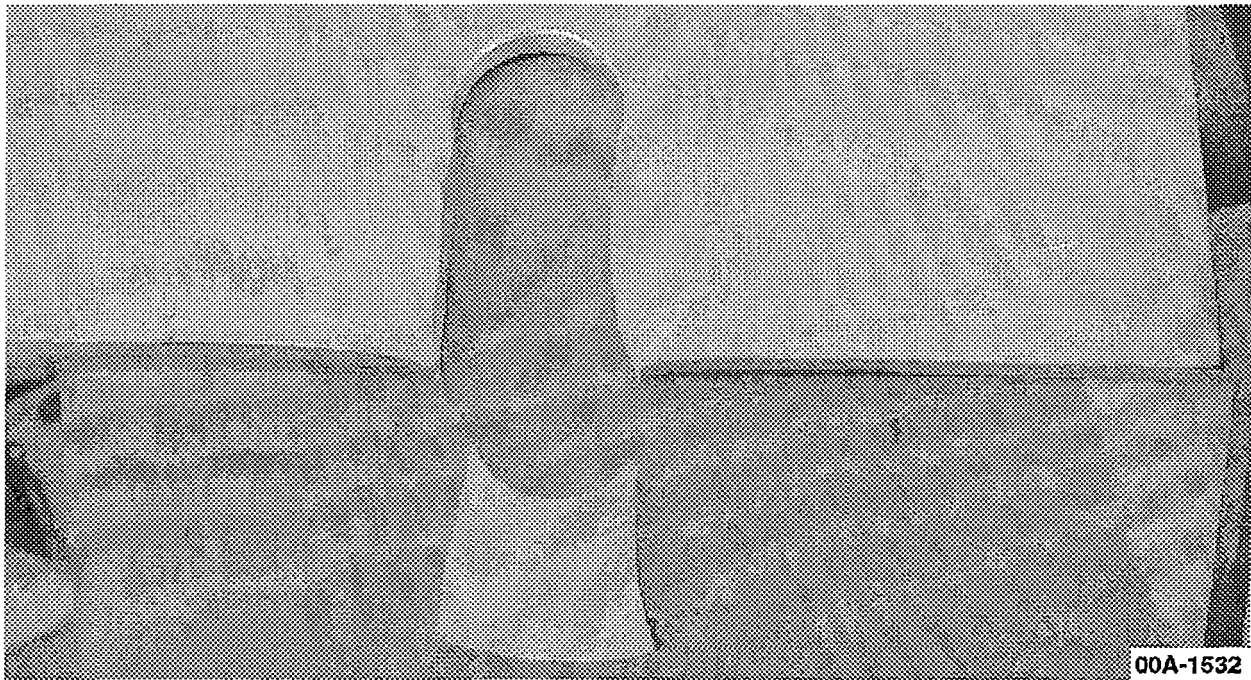


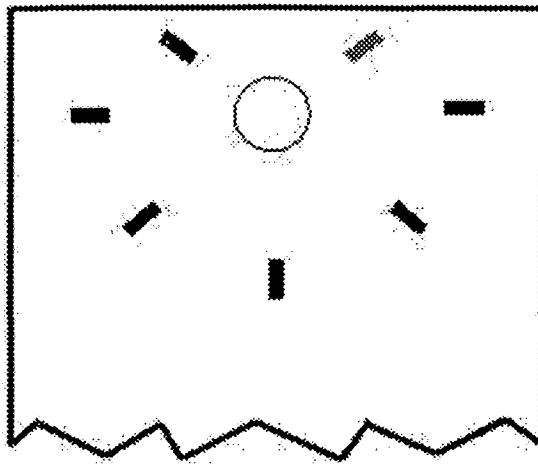
Figure 14. *Aluminum plate failed in shear while attempting to ramp the load to 20 kips*

where:

- ϵ_n = strain given by the silicon gauge on channel 'n'
- R_i = current setting resistor value (located on flex circuit) = 680Ω
- D_n = acquired data from channel 'n'
- D_i = silicon strain gauge output at zero strain
- G = circuit gain = 101
- R_{gn} = nominal resistance of channel 'n'
- GF_n = gauge factor at channel 'n,' typically around 108

The one channel that performed satisfactorily is highlighted in Figure 15. Strain data was collected during tension and compression loadings from both silicon and conventional strain gauges. The tension case results are shown in Figures 16 and 17 for the two types of strain gauges. Despite the noise in the output of the silicon gauge, its agreement with the conventional strain gauge is good. The noise in the output of the silicon gauge is due to the specific design parameters in the AMMI hardware, and will not be an issue in a properly designed circuit for the wheel/rail interaction force measurement. Note that the data from the silicon strain gauge is remotely transmitted by the RF link and collected by the computer, whereas the conventional strain gauge data is gathered through a hardwired connection.

The tension ramp test strain graphs are shown in Figures 16 and 17.



533-DTS-00023-4

Figure 15. Position of operational gauge on test piece during ramp load

The data from the compression tests are shown in Figures 18 and 19, respectively for the silicon and conventional gauges. Further work is needed to understand the discrepancy between these two curves.

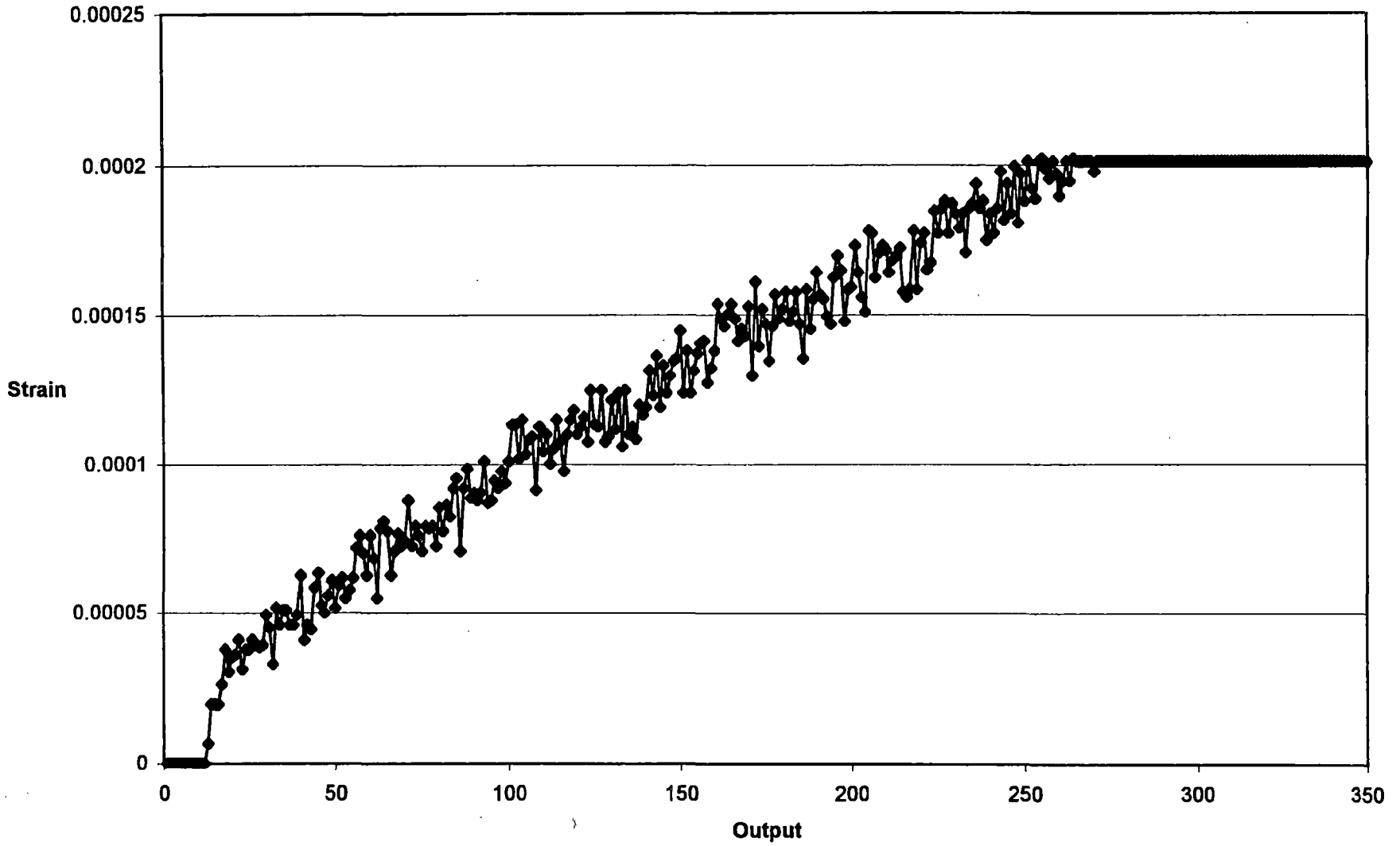
3.2.4 Fatigue Testing

When this hardware is subjected to the railroad environment, the loads it will experience will be cyclic. Therefore, cyclic tests should be performed. Since the initial test piece, the aluminum plate, broke during the 20 kip load test, a new test fixture was constructed. This new fixture consists of a 15 x 5 x 1/2 in. piece of steel and is shown in Figure 20. Instead of seven sensors, just one sensor of each type was used. A silicon strain gauge was mounted in the middle of the plate, shown in Figure 19. A standard strain gauge was mounted in the same position on the opposite side. The cyclic load was applied to the plate to compare the continuous responses from each sensor type. Just as in the ramp loading, the cyclic loading could only be run for about 30 sec due to limitations of the RF hardware.

The basic procedure in performing the fatigue test on the equipment is as follows:

- Place the plate in the Instron machine and apply a light load to hold the plate in place.
- Dial the load to the correct set point.
- Apply the pre-programmed cyclic loading to the specimen.
- Press the button on the flex circuit to activate the RF transmitter. It will stay active for about 30 sec.
- Monitor the specimen during cycling for cracks.

Test 1B, 10 Kips Tension, Position 6 (Channel 5), AMMI gauges

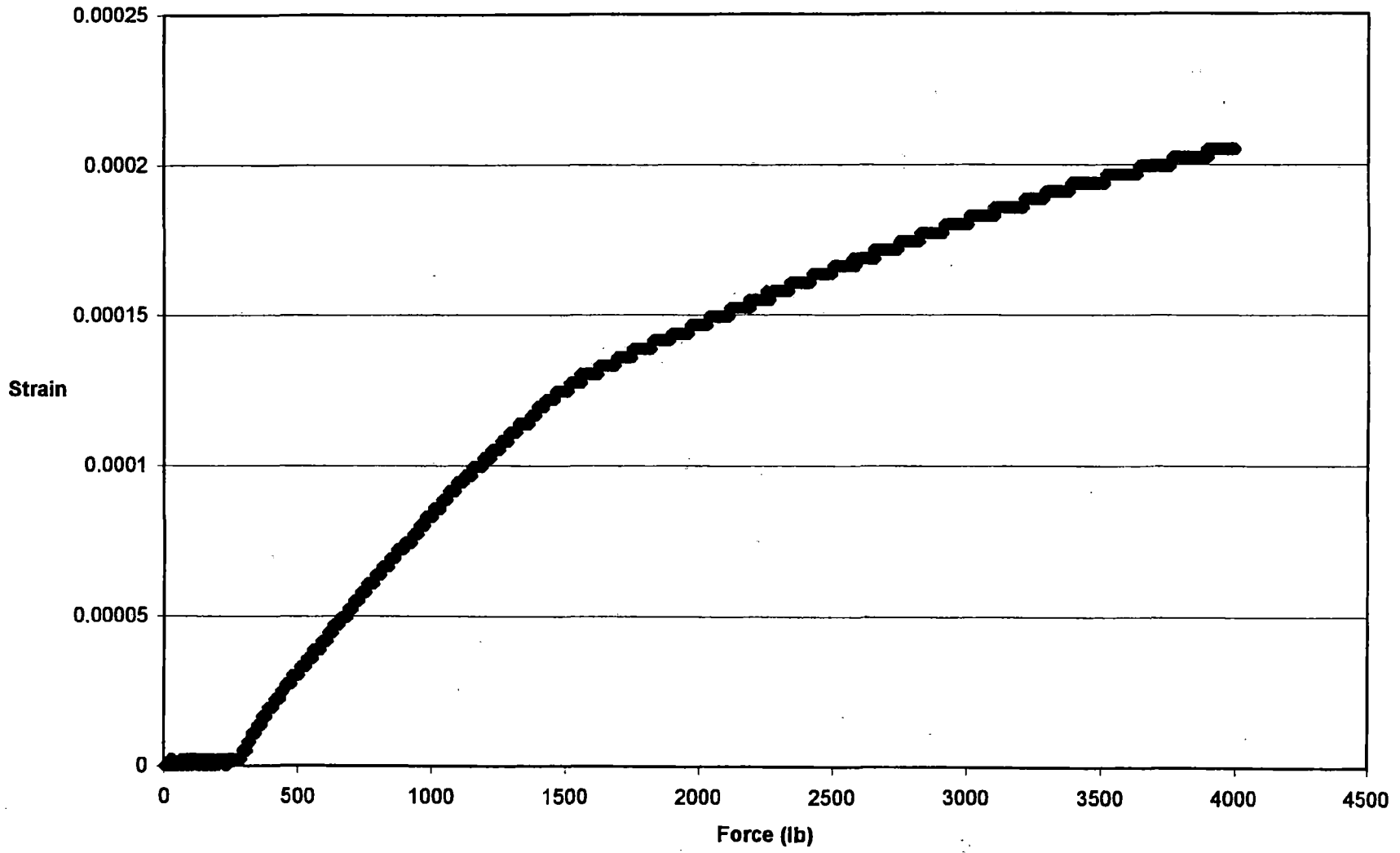


23

Figure 16. Silicon gauge tension test data up to around 4 kips

522-DTS-00023-5

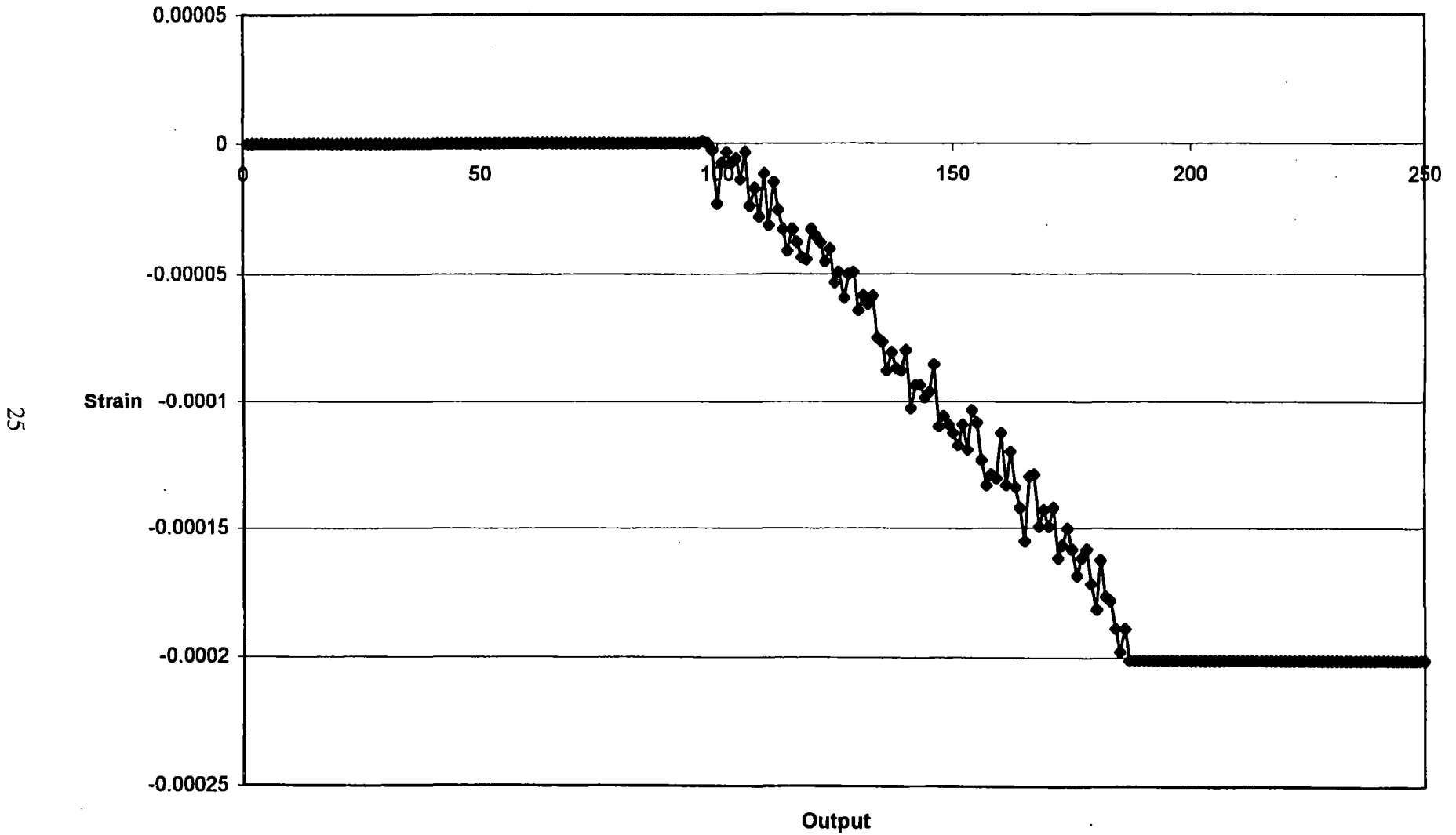
Test 1B, 10 Kips Tension, Position 6, Standard Gauges



24

Figure 17. Conventional strain gauge tension test data up to 4 kips

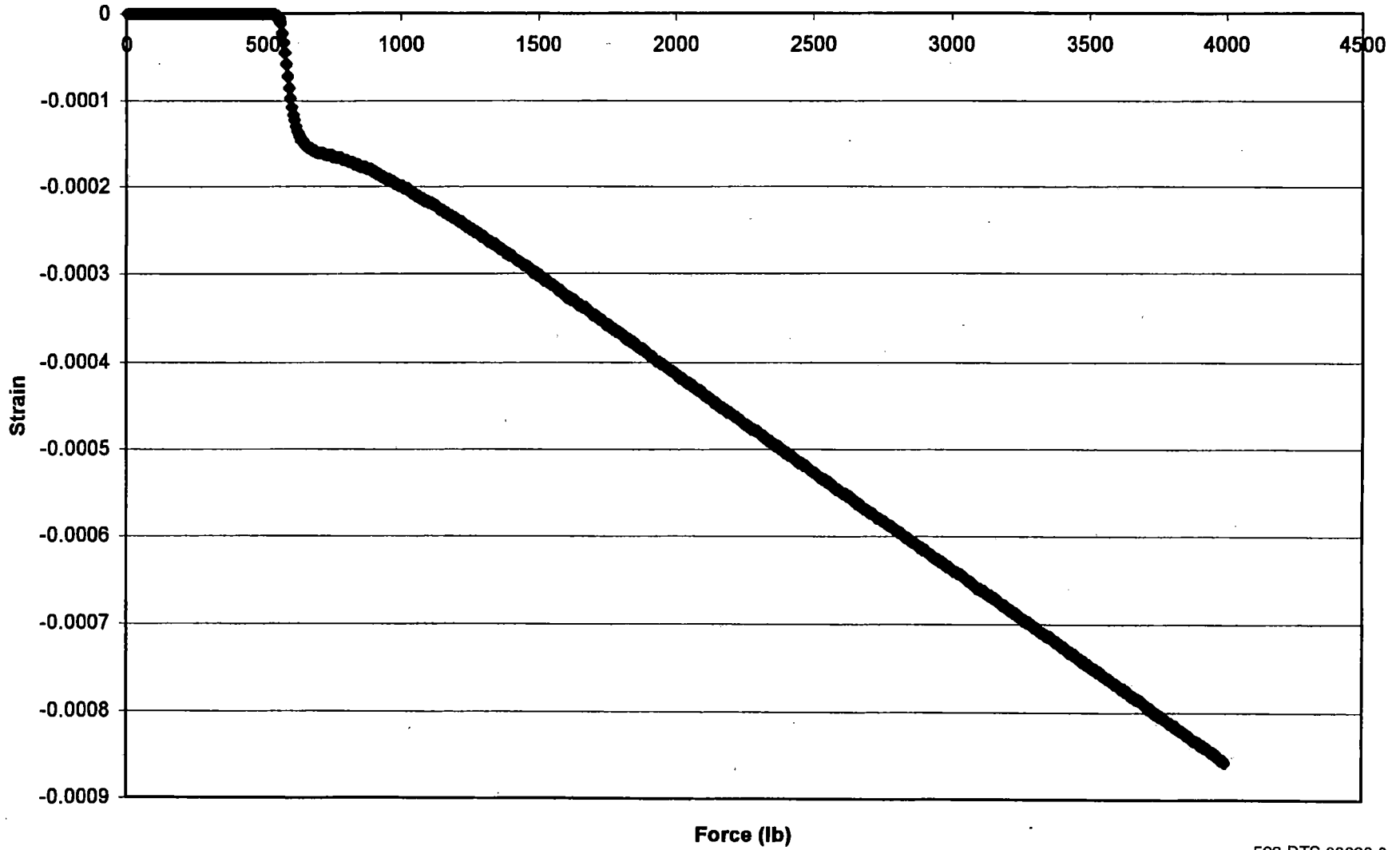
Test 1A, 10 Kips Compression, Position 6 (Channel 5), AMMI gauges



522-DTS-00023-7

Figure 18. Silicon gauge compression test data up to around 4 kips

Test 1A, 10 Kips Compression, Position 6, Standard Gauges



26

522-DTS-00023-8

Figure 19. Conventional strain gauge compression test data up to around 4 kips

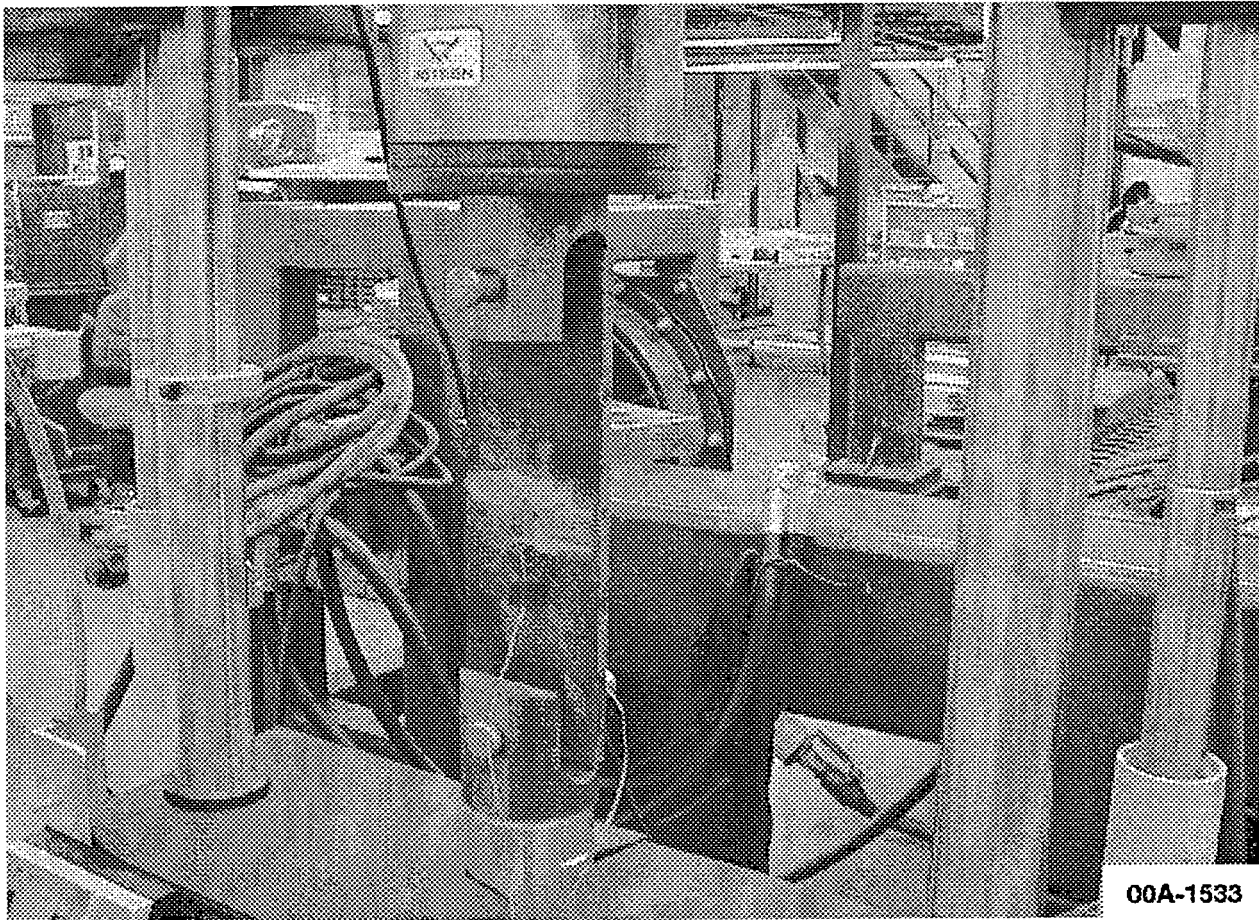


Figure 20. New steel test fixture loaded into Instron machine

- After the cycling program has ended, start the data acquisition program for the standard strain gauges.
- Apply the same pre-programmed cyclic loading to the specimen.
- Monitor the specimen during cycling for cracks.
- After the loading program has ended, stop the data acquisition program.

When the hardware is activated, it collects data for around 30 sec. During this period, a number of normalized voltages are collected. This number is usually around 550 and translates to approximately 18 points collected per second. To collect cyclic data and define a sine wave output properly, 10 data points per cycle are needed. Any less would not sufficiently define the wave's peak and trough. With this criteria, and the fact that the hardware outputs 18 points per second, only cyclic tests of around 1 to 2 Hz can be performed. If the sensor is placed 21 in. from the center of a rotating railroad wheel (which would be the outer edge of a 42 in. diameter

wheel), these frequencies correspond to a speed of 7.5 to 15 mph. For such a locomotive travelling at 100 mph, the frequency is around 13 Hz.

The first test performed was at 1 Hz, with a 2 kip setpoint and 1 kip amplitude. The results for the silicon gauges are shown in Figure 21. The standard strain gauges could not detect such small strains. This demonstrates one advantage of the silicon gauge over the conventional strain gauge, namely, sensitivity and is indicated by its gauge factor, which is a measure of a strain gauge's sensitivity. For a standard gauge, the factor is approximately two, whereas the gauge factor of the silicon gauges is nearly 100.

The peaks and troughs are still not as uniform as they should be, although there are enough points to properly define them. The noise in the signal input is not likely to be a serious issue, as a future circuit will be custom designed.

Another test was performed with the same load levels as the first, but at 2 Hz. Since the loads were equivalent as the first test, the standard strain gauges still could not detect such small strains. As was mentioned before, 10 points per cycle are needed to properly define a sine wave in a cyclic test. At 2 Hz, 20 points per cycle are required, since this particular hardware only outputs 18 per second. The noise in the data can be removed by a proper filtering process in a well-designed circuit. A graph of the results is shown in Figure 22.

The final cyclic test was performed at a higher load so that readings can be taken from the standard gauges and thus compared with the silicon gauge output. The experiment was performed at 1 Hz frequency, with a 10 kip setpoint and an amplitude of 5 kips. At 1 Hz, there would be enough data points from the equipment to properly define a cyclic output. The results from these tests are shown in Figures 23 and 24.

It is noteworthy that the strains are, in fact, relative strains. The reason for relative strains is as follows. The AMMI electronics, which collects data from the silicon strain gauges, resets itself each time it is activated by means of pressing a button. Resetting means that the output value representing zero strain is different for each reactivation because the Instron machine could be in the middle of a strain cycle when the button is pushed. Since at this initial point the real strain is set to zero by the AMMI electronics, the resulting measurements are relative strain.

**Cyclic Testing 1A Results (AMMI Gauges)
2 Kip Setpoint, 1 Kip Amplitude, 1 Hz Frequency**

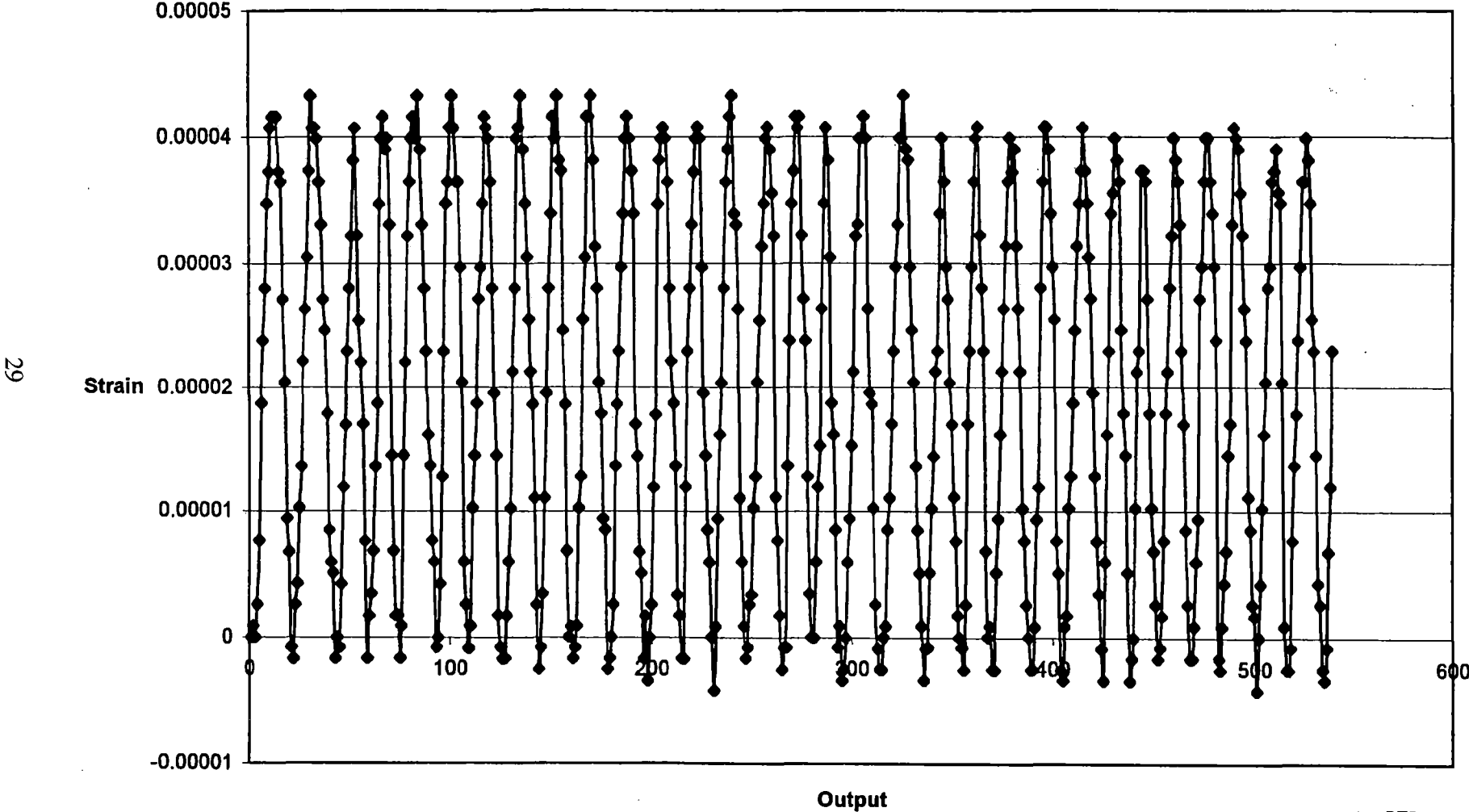


Figure 21. Results from silicon strain gauges in first cyclic test

**Cyclic Testing 2 Results (AMMI Gauges)
2 Kip Setpoint, 1 Kip Amplitude, 2 Hz Frequency**

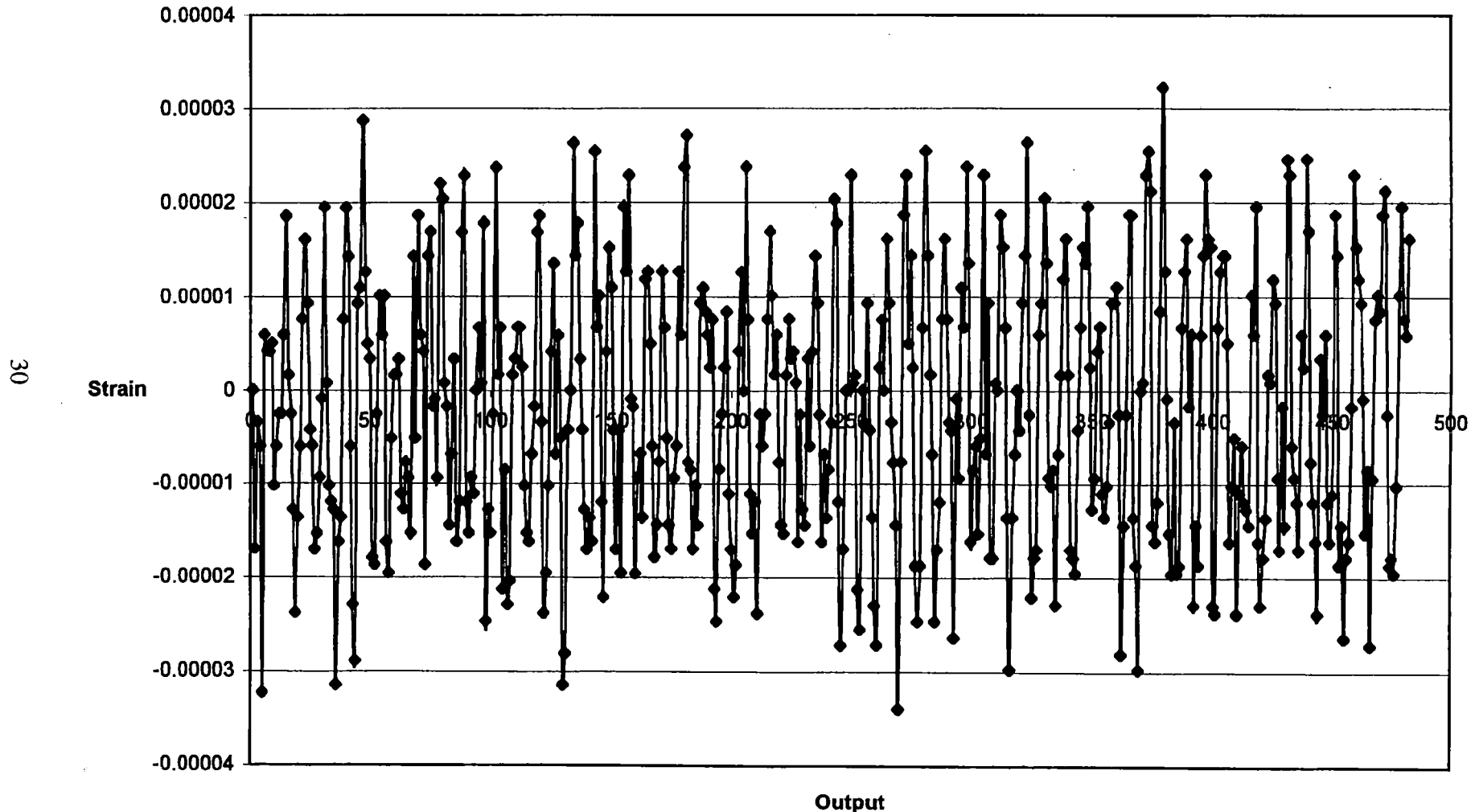


Figure 22. Results from silicon strain gauges in second cyclic test

Cyclic Testing 3 Results (AMMI Gauges)
10 Kip Setpoint, 5 Kip Amplitude, 1 Hz Frequency

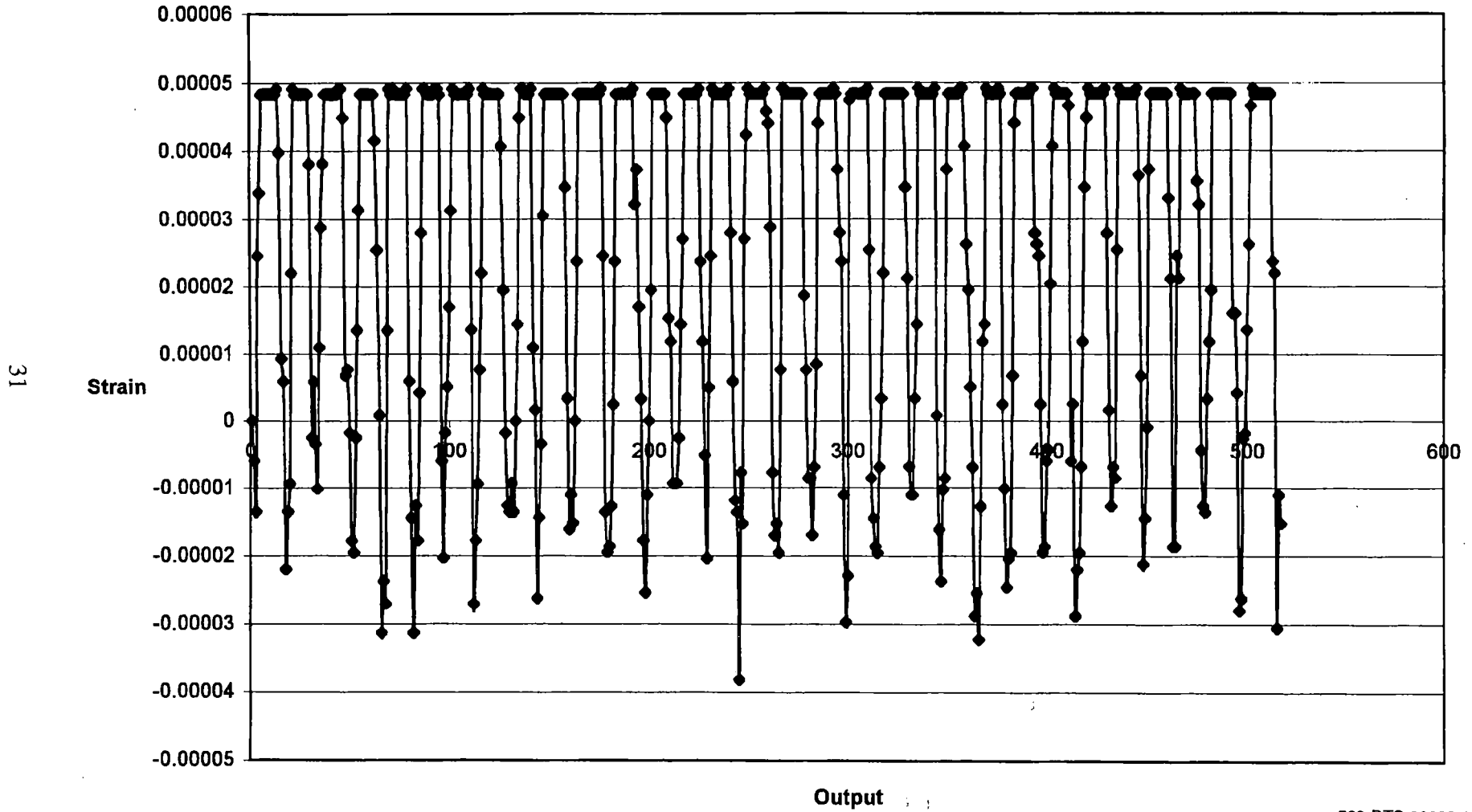


Figure 23. Results from MEMS gauges in third cyclic test

**Cyclic Testing 3 Results (Standard Gauges)
10 Kip Setpoint, 5 Kip Amplitude, 1 Hz Frequency**

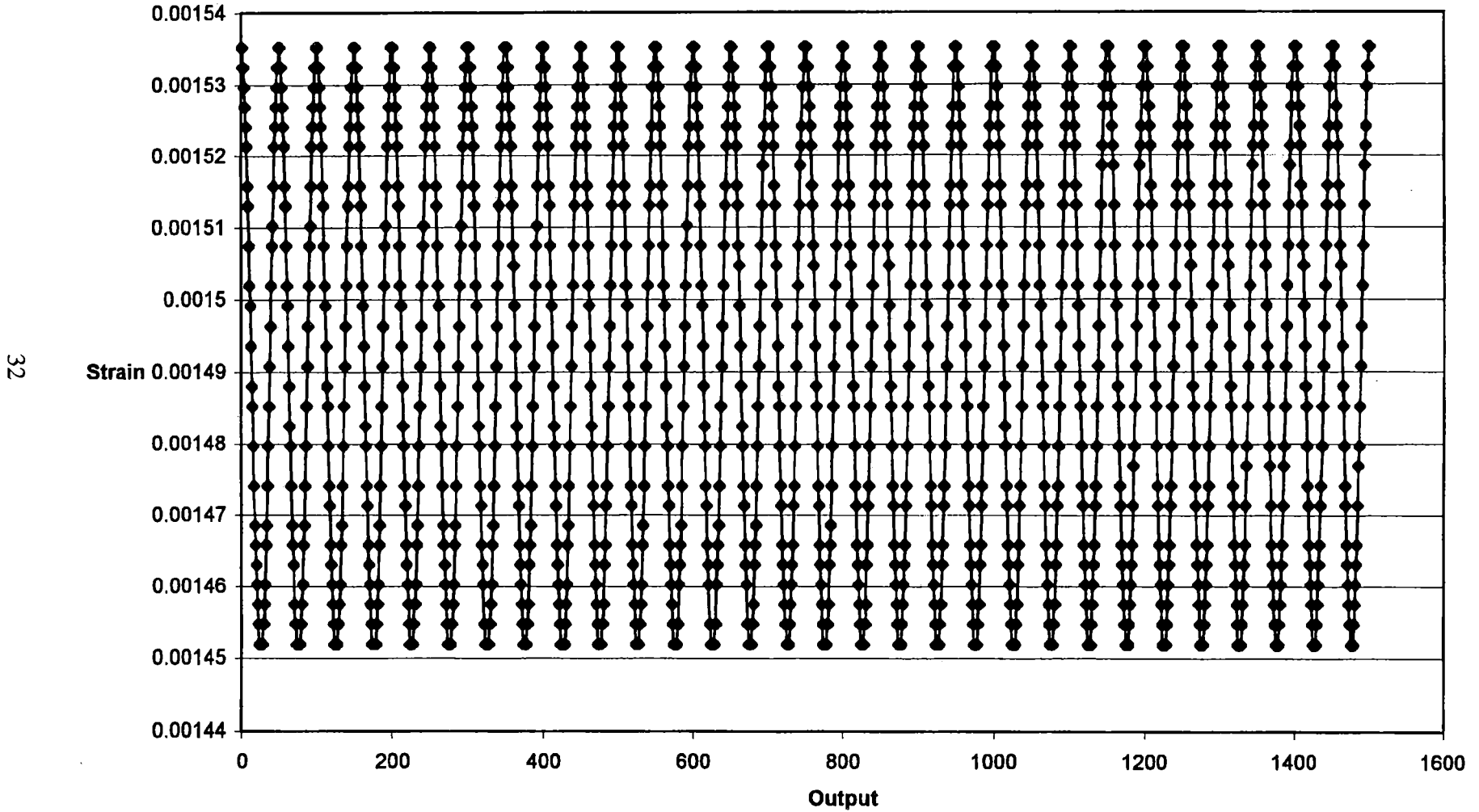


Figure 24. Results from standard strain gauges in third cyclic test

4. SENSOR CALIBRATION AND DATA EVALUATION METHODOLOGIES

Once the strain data is collected from the gauges, it is necessary to convert the data to force values. Present calibration methodologies are detailed and intensive. Foster-Miller is proposing the use of the innovative state-space analysis concept as a simpler alternative to the existing procedure.

The use of state space as a calibration methodology would provide further savings in these areas:

- Intensive finite element modeling of the wheel is not required.
- Precise gauge installation is not required.
- Calibration can be performed in the field.

4.1 Need for Calibration Methodology

Calibration of a wheel/rail interaction force measurement system is essential for proper data interpretation. Calibration consists of performing analyses or tests to determine the proper conversion factors between the strains that are output by the gauges and the actual forces that are experienced. The calibration procedure requires a significant portion of the total costs of existing instrumented wheel sets.

The state of the art in instrumented wheel sets is outlined in a patent entitled, "Instrumented Wheel Set System." (Patent 5,492,002) by the Association of American Railroads (AAR). The approach for the calibration of an instrumented wheel set assumed in this patent requires detailed structural finite element analysis, validation testing, further structural analysis, sensor installation and then calibration. The end result, although workable, is supported by a method, which is engineering intensive, and costly. Underlying this AAR method is the requirement to place sensors that are orthogonal to one another. Orthogonality means that the sensors respond to either lateral or vertical loads with minimal, if any, cross talk between sensors and with practically no time varying ripple in the output of each sensor. This method places a high requirement on the location accuracy of strain sensors.

4.2 Instrumented Wheel Set Calibration: An Example

In order to measure strain in railroad wheels, continuous strain data must be gathered to relate them to lateral and vertical force levels. All such strain measurement approaches need to clearly separate the effects due to lateral and vertical loads and minimize time varying ripple

from each sensor. Several methods to achieve this condition have been attempted. However, the most effective to date is that due to patent 5,492,002. All but one of the co-inventors are connected with the Association of American Railroads (AAR). The remaining co-inventor is with the Chicago Technical Center. Since most of the co-inventors are with AAR, this patent will be referred to as the AAR patent.

The AAR design approach uses the orthogonality of strain sensors located suitably on the wheel. The sums of squares of suitable sets of sensor readings should be nearly constant for a given force input, not depending on the rotary position of the wheel or on the force level in other directions. Fundamentally, the AAR wheel set design approach is one of identifying a geometrical configuration of sensor locations that maximizes orthogonality considering the detailed structural characteristics of the given wheel. To achieve this characteristic, the AAR approach relies on a very high level of structural analysis, careful sensor installation, and calibration. This high level of care is required to minimize two related error sources:

- Non-orthogonality, in which the aggregated readings from a set of sensors ripple as the wheel rotates, indicating a time-varying force when no such variation exists. The level of ripple constitutes additive measurement uncertainty.
- Cross talk, in which sensor readings reflect forces in nominally independent directions. Any uncorrected cross talk constitutes a measurement error.

This approach apparently is effective, obtaining desirably low levels of output ripple and cross talk. The AAR instrumentation method still requires a data acquisition computer and analysis capability to calculate the forces, correct for cross-talk, identify fault conditions, and identify unusual wheel-rail contact conditions, so the approach of pursuing maximal orthogonality per se has lost certain benefits.

The method described in this patent involves several steps. First, one must measure the wheel to determine its three-dimensional profile. This is an important initial step, since most railroad wheels are not necessarily simple in form and, thus, have complex mechanics.

After determining the topology of the wheel, a preliminary finite element analysis is undertaken to determine strain sensor placement. The wheel profile data serves as input to the finite element analysis program. According to the patent referenced above, "In either a new or worn case (i.e., wheel), the initial finite element model to analyze the subject wheel set is built using two-dimensional, axisymmetric elements representing a portion of the wheel. Each element can receive non-axisymmetric loads. The finite element model may typically use about eighty such elements, each being a second order, eight-node quadrilateral."

Nine loading conditions may be used as a minimum for this initial, finite element analysis calculation. By applying these loads, strain can be induced in the wheel plate. The resultant strains are then calculated around the circumference of the wheel and are related to wheel plate surface strains. The purpose of this exercise is to locate those positions on the wheel plate surface that are influenced by loads of one kind or another (e.g., either vertical or lateral loads).

With this surface strain mapping, another placement modeling is made to produce simulated sensor outputs to locate positions for strain sensors, which respond to only one type of load and have no, time-varying ripple in their output signals.

The above description glosses over many other calibration details that are included in the referenced patent. However, suffice it to say, that this approach requires considerable engineering effort and can be very costly. A new approach, called State Space, which eliminates these deficiencies and is advocated by Foster-Miller, is explained below.

4.3 Application of State Space Analysis

A new procedure for the calibration of instrumented wheel sets is proposed, which utilizes the concept of state space analysis. Using this approach, one performs less detailed structural analysis and installs sensors in positions approximating the ideal location, without the extremely high degree of analytical and experimental “tweaking” required in the AAR patent.

The key to this method involves the analysis of strain gauge data. If the relationships among wheel position, strain gauge readings, forces and contact position are known, then detailed strain gauge readings can be used to determine the operating conditions accurately.

In the state space approach, the output from each strain gauge is considered to be a coordinate in state space. The collection of all such coordinates leads to a multidimensional graph called state space. If there are sufficient inputs, each point in state space corresponds to a unique operating point (e.g., lateral/vertical forces, wheel contact position). With a suitably large database for which the operating points are known, the state space is well populated. One may interpolate any new operating conditions from previously encountered neighboring conditions.

There are several advantages of using state space for calibrating instrumented wheel sets. Intensive, costly engineering is traded for data analysis that can be automatically performed by computer. With the availability of high powered, lap top computers, this tradeoff may be considered favorably. A large calibration database is not necessary. Redundant strain gauge data can be used to check consistency among all gauges. Problematic gauges can be “flagged” to determine if a malfunction is intermittent, permanent, or a failure mode that produces skewing of the data.

4.3.1 Applying State Space Analysis to Force Measurement

The desired performance attributes for an instrumented wheel set system are the ability to accurately determine the forces and locations of the contact point between a wheel and rail as functions of time/position. The instrumented wheel set system described in the AAR’s patent achieves these attributes through highly detailed structural analysis, validation testing, further detailed structural analysis, sensor installation, and calibration. Although effective, this approach is not cost-effective. A more promising approach would be to replace much of the up-front detailed engineering effort with on-line analysis of sensor data. This should obtain performance attributes that are at least as good as those of the AAR wheel set, but at a fraction of

the cost. This approach would be applicable with any type of strain gages (conventional or silicon strain gauges) and any means of communication (slip ring or RF).

An alternative approach is to perform a less detailed structural analysis and to install the sensors in positions approximating the ideal, but without the extremely high degree of analytical and experimental “tweaking” used in the AAR approach. If one were to aggregate the readings of such a wheel in the way that AAR does, one would expect to obtain an undesirable level of ripple and cross talk. However, with the capabilities of modern computers, the sensor readings could be corrected to a very high degree through analysis. In fact, this approach could obviate special machining of the wheel, except to clean the locations where the sensors are to be attached. Considering the relative cost of engineering/technician labor and a marginal amount of computing power, this should be a highly favorable tradeoff.

The key to this alternative approach is in the analysis of the strain gage data. The principal characteristic of the AAR approach is avoiding a need to consider the rotational position of the wheel. In reality, the cyclic variation in the output of each individual strain gage reflects the wheel position. In the presence of steady forces, each of the strain gage outputs is essentially a wheel position “clock,” with an angular offset corresponding to the strain gage location. Even with significantly varying forces, the overall information available from all of the strain gage outputs would provide an extremely accurate indication of wheel position. Thus, if the relationships among wheel position, strain gage readings, forces and contact position are known, the detailed strain gage readings can be used to determine the operating condition accurately.

The relationships among wheel position, strain gage readings, forces, and contact position are usually nearly linear, since the loading on the wheel plate is elastic. In fact, the AAR approach assumes linearity, and that any nonideal sensor location can be corrected using a (linear) correlation matrix. Thus, it would be possible to develop a straightforward linear analysis that combines a wheel position indication and the strain gage readings to produce a maximally accurate estimate of the forces and location of the contact point. At the same time, some aspects of this problem are nonlinear, such as the potential for a given strain gage to fail, an amplifier to drift, or for a two-point wheel-rail contact to occur. These disparate behaviors could be handled, as AAR has done, by supplementing a linear analysis with a nonlinear error analysis. Alternatively, it may be advantageous for the entire analysis to be performed nonlinearly. In the nonlinear approach, no basic form is assumed between the inputs and outputs. Instead, a framework is created that permits the actual relationships between the inputs and outputs to be characterized and understood. In our work with nonlinear systems, we often use two different types of nonlinear analysis techniques. These are explicit state space techniques, and implicit neural network techniques, both of which are described below.

The use of neural networks has grown in popularity in recent years, because they permit nonlinear correlations to be performed without requiring a high degree of detailed analysis. Although a full discussion of their behavior and attributes is beyond the scope of the current discussion, neural networks have the following salient characteristics:

- In principle, they permit an arbitrarily nonlinear relationship between inputs and outputs to be determined without assuming a particular form for the relationship.

- They determine this relationship through a process in which sets of inputs and the corresponding outputs are used to “train” the network.

Because the network training process is pseudo-random in nature, it is not possible to determine whether the “best” network has been found. A level of confidence about network maturity can only be gained through repeated training runs with different initial conditions (randomly selected).

Given a new set of inputs, there is no way to determine whether it is similar to any of the input sets used to train the network. If an input set represents a novel operating condition, the network will produce an output without providing an indication that there is anything unusual about the data. Thus, for a neural network to be useful in a critical application, its training set must include data for all foreseeable operating conditions, including all error states. There are special neural networks that can be used as “novelty detectors,” but they have the unfortunate tendency to consider many normal conditions as novel (producing false positive error indications).

This difficulty of identifying abnormal operating conditions gives us cause for concern about the use of neural networks in this application. In particular, if a fault condition arises that is difficult to model in training (such as unusual form of intermittence of a strain gage output), the network may produce incorrect force predictions. Further, it is difficult to determine whether or not a given strain gage output is normal using a neural network, without having access to extensive field data covering a broad range of normal and abnormal conditions, including force transients that are unusual but real.

These difficulties lead us to prefer the alternative approach of explicit state space analysis. In explicit state space analysis, the inputs (e.g., strain gage outputs) are used as coordinates in a multi-dimensional graph, called the state space. If there are sufficient inputs, each point in the state space corresponds to a unique operating condition. Thus, there are one or more output values (e.g., forces and contact point location) that are uniquely determined by the location of each state space point. As one moves from point to point in the state space, the output values vary smoothly and continuously. Thus, if one has a sufficiently large calibration database of conditions for which the operating state is known, the state space is well populated, and one can interpolate any new operating condition from previously encountered neighboring conditions. By characterizing the level of confidence in each sensor reading, corresponding to a likely range of error in state space location, one can easily obtain an indication of the error associated with a given measurement. This overall approach is called state space analysis. We have extensive experience using it in applications ranging from diagnosing the condition of rotating equipment to the active control of helicopter vibrations.

One does not need a very large calibration database to build a state space analysis system, because the responses of the sensors vary linearly with the wheel loads. For example, one could perform a set of calibration tests on the instrumented wheel, applying vertical and lateral loads and varying the location of the contact point for many angular positions of the wheel. This limited group of data could then be scaled linearly to populate the state space with a very broad

range of operating conditions. One could limit the scaling of the calibration database to conditions that would represent reasonable force levels, avoid amplifier saturation, etc. This way, any new conditions that are encountered (i.e., new sets of sensor readings that are not located near any points in the state space) could be flagged as likely error conditions requiring further analysis.

It is an understatement to say that the strain gage outputs are sufficient to define the loads on the wheel and the contact point location. In fact, there is a great deal of redundant information present in the data, which can easily be used to check the consistency of the strain gage outputs against one another. For example, multiple strain gages will usually be positioned in a way that renders them sensitive to the vertical load on the wheel. The variation of such strain gages relative to one another can be compared with their normal variations to indicate whether all are sensing the same phenomenon. If not, it is straightforward to determine which gage or combination of gages are not functioning properly. The reduced set of properly functioning gages can then be used to obtain the best available determination of the wheel operating condition. By examining the variation of the operating condition in the state space directions corresponding to the “bad” sensors, an indication can be obtained of the error level associated with the measurement. The problematic gages can then be flagged and monitored to determine whether a given malfunction is permanent, intermittent, or constitutes a failure mode that produces a skewing of the sensor output. By a process of continually checking the consistency of sensor outputs, the skewing of one or more sensor outputs can be accommodated, and the analysis can “heal” around it. Thus, an explicit state space analysis can be fault indicating, fault-tolerant, and self-healing. This analysis can be quickly updated using new calibration data.

4.3.2 Example of State Space Analysis

By replacing much of the labor intensive analysis and “fine tuning” of the AAR approach, the state space approach should provide all of the benefits of an accurate and robust instrumented wheel set at a very reasonable cost. To illustrate this alternative approach to developing an instrumented wheel set system, let us examine a simplified version of the problem, in which only the lateral and vertical forces are considered. There is nothing about the technique that limits it to two forces (or three or four, for that matter), but this will illustrate the key points in a simplified system.

We performed a simulation of this simplified system using the Matlab programming environment, along with a proprietary Matlab-callable state space prediction routine. This routine performs a local state space prediction algorithm based on a k-delta tree nearest-neighbor search algorithm, and was developed for a recent program Foster-Miller performed for the U.S. Navy on controlling helicopter vibrations. This capability is not broadly available, even within the nonlinear dynamics community. Our simulation of an instrumented wheel set was based on the following assumptions described below.

There are four sensors for each force direction, for a total of eight in this example. There is no particular limit to the number of sensors that are used, except that there must be a sufficient number. Using a very large number of sensors could result in an undesirably high cost for instrumentation, but this would not affect the feasibility of the analysis.

For each force direction, half of the sensors are nominally sensitive to the sine of the wheel position angle, and half to the cosine of the angle. Although the AAR approach requires the sensors to be placed with high precision to ensure the orthogonality of sensor pairs, this is not the case in this example. Thus, we can accommodate a significant level of error in sensor placement.

The sensors are located geometrically with angular position errors randomly chosen over a circumferential range of ± 5 deg. Although this arrangement would be a terrible level of accuracy in the AAR approach, this example will demonstrate the lack of sensitivity of State Space approach to such errors.

The amplitude sensitivity of each sensor may differ from a nominal value of unity by as much as 10 percent. The AAR technique would be hard-pressed to accommodate such a large error, but this will demonstrate the flexibility of the current technique.

The cross talk between the vertical forces and lateral sensors (and similarly for the lateral forces and vertical sensors) may be as high as 10 percent. There is no fundamental limit to the cross talk that can be accommodated, but numerical inaccuracy could creep into the analysis if the cross talk were large.

The wheel set would be calibrated by applying known lateral and vertical forces for different rotational positions of the wheel, permitting the sensor gains and phase angles to be determined.

The gain and angular position errors were selected at random, resulting in the values shown in Table 6. Although the amplitude and phase angle errors in the real problem are related, the simulation does not reflect this fact. We did not bother to model this phenomenon, because it has no influence on the accuracy of the results (because the analysis does not assume that the forces and sensor responses are linearly related).

Next, we chose somewhat arbitrary time profiles for the vertical and lateral forces. We assumed that the forces were steady for 100 readings at a time, and then changed to another

Table 6. Gain and phase error values used in simulation

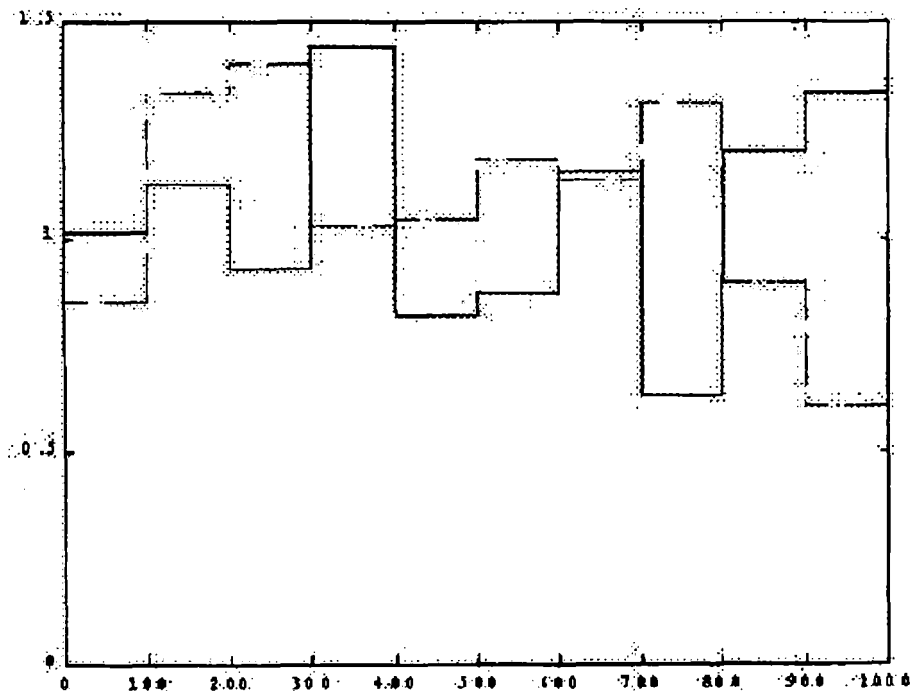
Nominal Force Sensed	Sensor No.	Vertical Force Gain	Lateral Force Gain	Vertical Force Phase Error (deg)	Lateral Force Phase Error (deg)
Vertical	1	1.0360	-0.0987	-3.7395	0.7790
Vertical	2	0.9323	-0.0872	1.5962	2.1476
Vertical	3	0.9337	-0.0020	-0.6020	3.3517
Vertical	4	0.9103	-0.0509	1.3499	-2.0531
Lateral	5	-0.0435	0.9219	-4.5011	-1.5347
Lateral	6	-0.0386	0.9649	3.3516	-2.7102
Lateral	7	0.0130	0.9917	2.6455	-0.2372
Lateral	8	-0.0126	1.0681	-1.5742	-2.1293

randomly selected steady level, and so forth. In this simulation, the reading interval is such that 360 readings comprise one rotation of the wheel, so the steps between force levels are not related to the wheel position. We selected this type of profile to demonstrate the following:

- Results do not depend on a smooth variation of the forces with time.
- Wheel position has no bearing on the force measurement.
- Vertical and lateral forces can vary arbitrarily relative to one another.

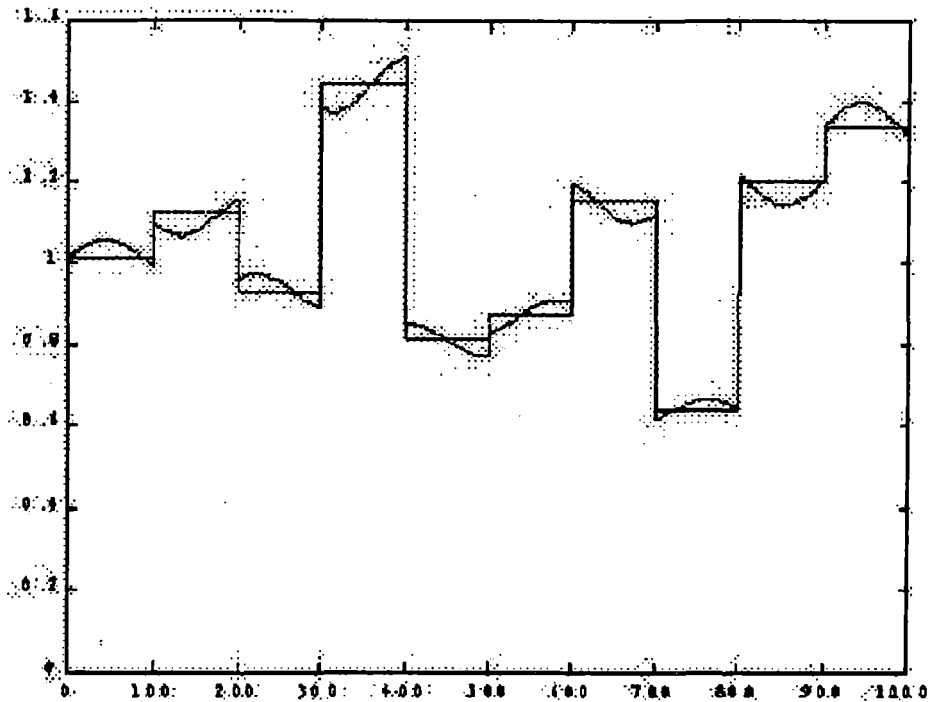
Figure 25 shows the force profiles that were used. The vertical force is represented by the solid line, and the lateral force by the dashed line.

Before proceeding to the state space simulation, let us examine the results that would be obtained if a linear analysis were performed using the assumptions of this simulation. In principle, a linear analysis could account for the gain errors of each of the strain gages and the cross talk between force directions, so let us assume that these errors can be accommodated exactly. The inherent assumption of a linear analysis is that the sensors are orthogonal. Thus, although the wheel position is unknown (so the angular dependence of each sensor cannot be accounted for), the sum of the squares of any pair of orthogonal sensors should be proportional to the square of the corresponding force. Figure 26 illustrates the vertical force that is predicted when the outputs of sensors No. 1 and No. 2 are combined after eliminating amplitude and cross talk errors. As the figure shows, the actual and predicted forces are of the same level, but the predicted force varies during each of the fixed steps in the actual force. The standard deviation



522-DTS-00023-13

Figure 25. Force histories used in simulation



522-DTS-00023-14

Figure 26. *Vertical force predicted assuming orthogonality of sensors No. 1 and No. 2*

of the error in this figure is 3.36 percent of the average force level. Taking two standard deviations as our standard for accuracy, the lack of orthogonality of this sensor setup causes a linear analysis to produce a level of uncertainty of 6.7 percent of reading.

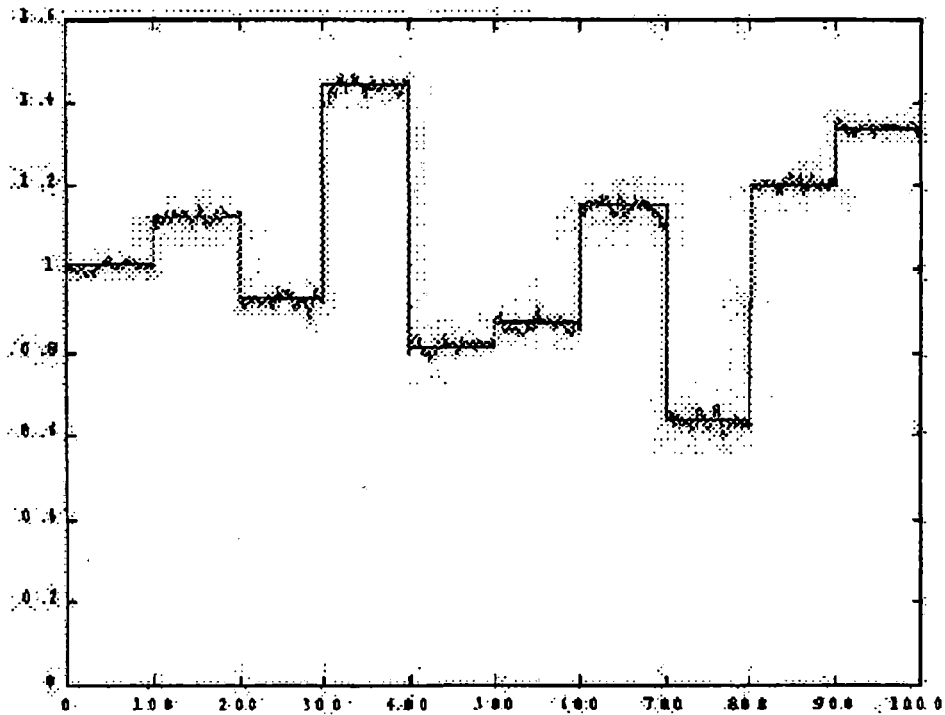
Our approach to analyzing the sensor data, allowing for the peculiarities of our simulated instrument setup, is to construct a state space in which the “directions” are readings from each sensor. Thus, in this case, the state space has eight dimensions. There are values of vertical and lateral force that correspond to each point in this state space. Once this state space is constructed from calibration data, it can be used to “look up” the forces for a given set of new sensor readings. Since the response of a given sensor to any combination of forces is a linear sum of the responses to the individual forces, we can use the calibration data to calculate what the sensor response would be for an arbitrary combination of forces. Our strategy is to construct the state space for many combinations of forces and wheel positions, so that any new set of sensor readings is near a previously calculated condition. The forces predicted for the new sensor readings are then calculated as maximum-likelihood values based on the neighboring values in the state space.

There are many potential strategies for selecting the points to be used in constructing the space. For this simulation, we picked a relatively poor one, using 10,000 points with the vertical and lateral forces and wheel rotational position selected at random. This amount may seem like a large number of points, but if each of the three variables (two forces plus position) is independent, a space constructed of 10,000 points is equivalent to roughly 22 independent values

of each variable, a fairly sparse sampling. For example, visiting only 22 phase angles would be equivalent to a spacing of about 16 rotational degrees between calibration points.

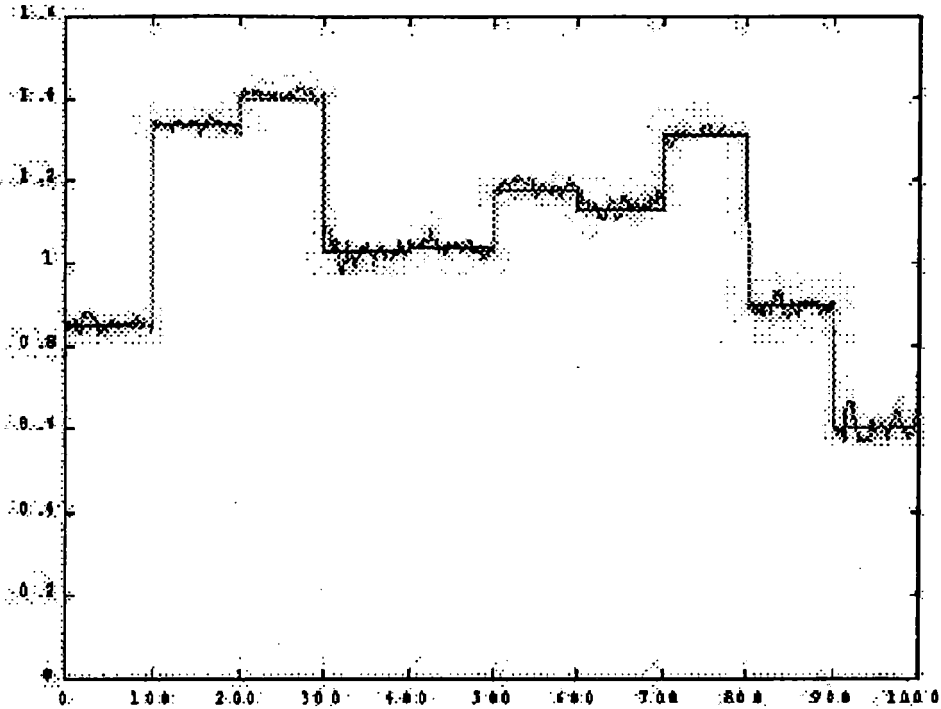
Figure 27 illustrates time histories for the actual vertical force and that predicted using the state space prediction technique. As the figure shows, the prediction tracks the actual forces quite closely. The standard deviation of the error is 1.32 percent of the mean force level, so the level of uncertainty is approximately 2.6 percent of reading. Much of the error comprises rapid “jiggles” around the actual reading: if one had an idea of the rapidity with which the forces actually change in practice, low-pass filtering of the predicted forces could significantly reduce the predictive error. Figure 28 illustrates the corresponding result for the lateral force prediction. In this case, the prediction uncertainty is approximately 2.9 percent of reading, still an excellent result.

In order to test the sensitivity of this approach to noise, we repeated the analysis shown above using sensor readings that were contaminated with random noise of 1 percent of the signal amplitude. Graphs of the result appear identical to Figures 27 and 28. The uncertainty in vertical force is increased only slightly, from 2.6 percent to 2.7 percent of reading, and similarly for lateral force (from 2.9 percent to 3.0 percent of reading). Thus, the predictive accuracy is not unduly sensitive to noise. This should not be surprising, since the eight sensor readings contain significant redundant information: noise in one sensor tends to cancel noise in another.



522-DTS-00023-15

Figure 27. State space prediction of vertical force



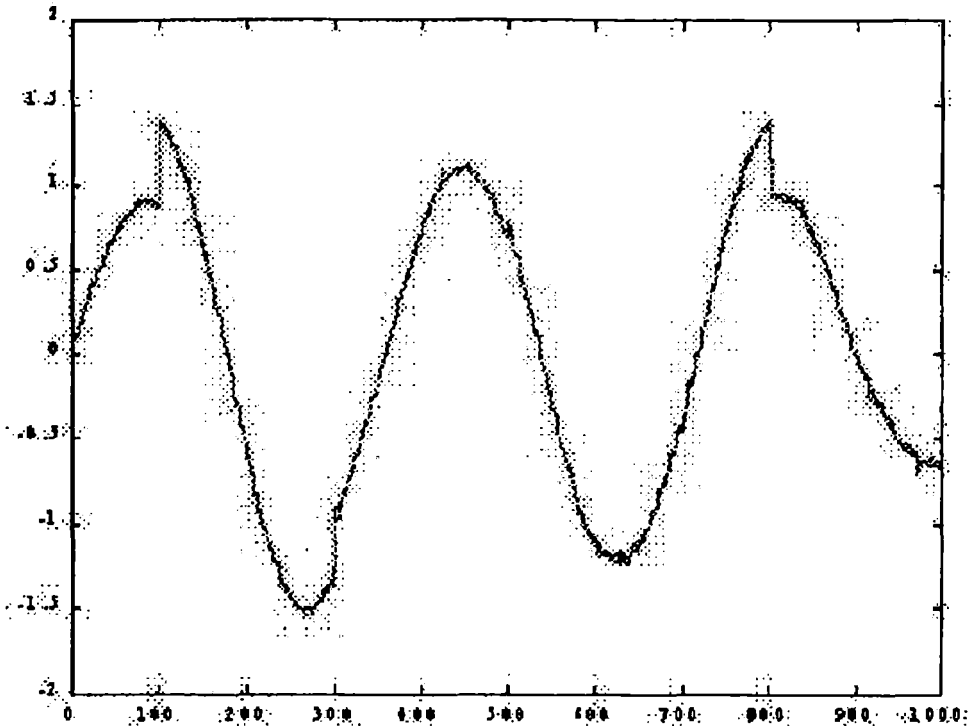
522-DTS-00023-16

Figure 28. State space prediction of lateral force

There are two additional points in particular that should be made about the state space analysis:

- Using a desktop computer, each force prediction for this simulation required approximately 1.3 msec. Our experience with real-time applications of state space analysis indicates that fast-embedded processors are typically capable of performing this analysis much more quickly than a desktop computer. Thus, one could perform significant state space analysis and still obtain responsive force measurements with modest computing hardware.
- We have found in other state space analysis efforts that the prediction accuracy is strongly affected by the way the database used to construct the state space is selected. Significant improvements in prediction accuracy can accrue by selecting the state space points carefully. We have developed methods to do this, but purposely did not apply them here. Thus, the results presented here can be considered a lower bound for the potential accuracy achievable through suitable development.

The other key capability that can be demonstrated with this simulation is that the redundancy of the sensor readings can be used to check the status of each sensor. One way of achieving this would be to use the other sensor readings to predict the reading of each sensor in turn, and to compare these predictions to the actual sensor readings. Figure 29 illustrates this idea, graphing the actual time trace for sensor No. 8 along with the behavior for sensor No. 8 that is predicted



522-DTS-00023-17

Figure 29. *Actual and predicted time traces of signal for sensor No. 8*

using sensors No. 1 to 7. The occasional jumps in the traces reflect the step changes in the vertical and lateral forces. As the figure shows, it is not easy to distinguish the actual and predicted readings. The level of uncertainty between the two traces is 3.3 percent of reading amplitude. Clearly, there is no reason to believe that there is any fault in sensor No. 8. This process could easily be performed with all of the other sensors, indicating the degree to which each is consistent with the others. When a sensor is found to be inconsistent with the others, it could be flagged and not used in making force predictions. The nature of the sensor fault could then be characterized by determining whether the inconsistency is a matter of a gain error, phase error, a fixed sensor level (e.g., instrument failure), or an intermittent failure. It would be fairly straightforward to extend this technique to the possibility of multiple sensor failures. This type of consistency check could be performed as a background process of the main force calculation process, resulting in a seamless, self-checking instrument system that achieves desirable accuracy at reasonable cost.

4.3.3 Prior Use of State Space Analysis at Foster-Miller

The use of state space analytical techniques for the calibration of railroad wheel measurement sets fits well with Foster-Miller's initiative in nonlinear dynamics, which we have been pursuing for several years to apply recent developments in the methods of nonlinear dynamics to practical engineering applications.

To gain a strong basis in the fundamentals of nonlinear dynamics, we have formed a partnership with Applied Nonlinear Sciences, LLC, a company formed by four researchers from the Institute for Nonlinear Science at the University of California at San Diego. These researchers have been responsible for developing many of the more practical methods of analyzing and controlling nonlinear dynamical systems, essentially enabling the practical application of this technology. The body of work by our partners in nonlinear dynamics is very extensive, including many technical papers in refereed journals covering basic methods of identification, characterization, prediction, synchronization, and control.

Our partnership with Applied Nonlinear Systems, called Enhanced Dynamics, is intended to develop and apply joint intellectual property to new applications of nonlinear dynamics. This partnership has been responsible for the development of several useful analysis tools. Current and recent programs that fall within our initiative in nonlinear dynamics include the following:

- *Reduction of helicopter vibrations using chaotic control.* This recent Phase II SBIR program for the U.S. Navy (NAVAIR Systems Command Aircraft Division, date of completion March 1999, Julieta Booz, COTR, 301-342-8574) used a state space representation of helicopter vibrations to improve an existing system for actively isolating a helicopter airframe from rotor-generated vibrations. Our commercialization partner for this effort was GKN Westland Helicopters, a UK manufacturer of helicopters. Westland's EH-101 Merlin helicopter is the first production helicopter to incorporate an active vibration control system, a system which they call Active Control of Structural Response (ACSR). The existing ACSR system is based on an adaptive linear control approach, and achieves a first-order reduction in airframe vibration. Still, the existing ACSR system is limited in the extent to which it can reduce vibration, because the rotor vibrations vary irregularly with time. Our analysis of recent ground-based tests indicates that we should be able to achieve a two-fold improvement in RMS airframe vibration amplitude, close to the theoretical limit of controllability of the aircraft. The recent Phase II effort culminated in a real-time demonstration of the key control system capabilities in a ground test rig.
- *Dynamical Instruments.* In a previous Air Force Phase II SBIR program (U.S. Air Force Phillips Laboratory SBIR, terminated May 1994, Lt. Eric Critchley, COTR), we developed a method of relating the irregular variation of a sensor signal to the operating conditions that produced them. The problem addressed in that particular program was the measurement of liquid-gas two-phase flows using an ultrasonic measurement of the liquid film thickness on the tube wall. By relating the irregular variation of the film thickness to the flow conditions, we found that we were able to determine both the liquid and gas flow rates with very desirable accuracy. This method, which we call Dynamical Instruments, has proven to be fairly fundamental and generally applicable, resulting in three U.S. patents to date (Patent Nos. 5,600,073, 5,714,691, and 5,741,980) and several additional U.S. and foreign patents pending.

4.4 Calibration Hardware

It will be necessary during the Phase II program to develop hardware to provide in situ calibration loading to the train wheel to provide calibration references to the state space analysis system. The equipment shall have these primary characteristics:

- The equipment must have the ability to apply lateral and vertical loads to the wheel that has the measurement system mounted to it.
- The calibration equipment must be able to apply these loads in the field, eliminating the need to perform the calibrations in the shop.
- The system must be easily portable, so it can be transported and implemented at any location in the field.

These guidelines will be used to perform the design of this equipment in Phase II.

5. CONCLUSIONS

The following is a list of goals that were accomplished during this Phase I program:

- A new cost-effective and efficient approach for the measurement of wheel/rail forces was investigated. This has advantages over the conventional method and does not require slip rings and hand-installation of the gauges. The gauges also do not require the precise placements that are presently required.
- Silicon strain gauges were evaluated under loading conditions on the order of those seen in the railroad environment. Despite some initial hardware difficulties, the gauges performed comparably to conventional foil gauges. In fact, at lower load levels, the silicon gauges showed better sensitivity and resolution of strain.
- RF data transmission hardware was demonstrated to successfully transmit data from the signal conditioning hardware to the data collection computer while retaining signal quality.
- An innovative calibration method using state-space analysis was outlined. This process has the potential to dramatically reduce the cost and labor that are presently necessary for the calibration of instrumented wheel sets.

2176: Advanced Railroad Wheel/Rail Interaction
Force Measurement System

03-Rail Vehicles & Components

PROPERTY OF TRB
RESEARCH & DEVELOPMENT
LIBRARY